Title
DISPERSION OF GASEOUS MISSIONS FROM A GROUND-LEVEL LINE SOURCE

Authors
Winges, Kirk D.
Grens, Edward A.
Vermeulen, Theodore.

Publication Date
1973-11-19

LBL-2444

DISPERSION OF GASEOUS EMISSIONS FROM A GROUND-LEVEL LINE SOURCE

Kirk D. Winges*, Edward A. Grens II and Theodore Vermeulen

November 19, 1973

Prepared for the U. S. Atomic Energy Commission
under Contract W-7405-ENG-48

*Filed as a M.S. thesis

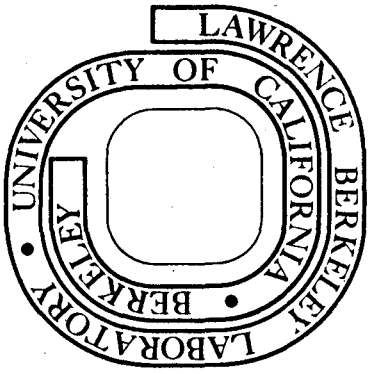

LBL-2444

DISCLAIMER

LBL-2444

UNIVERSITY OF CALIFORNIA
Lawrence Berkeley Laboratory
Berkeley, California

AEC Contract No. W-7405-eng-48

DISPERSION OF GASEOUS EMISSIONS FROM A GROUND-LEVEL LINE SOURCE

Kirk D. Winges*, Edward A. Grens II, and Theodore Vermeulen

Energy and Environment Division
Lawrence Berkeley Laboratory
and
Department of Chemical Engineering
University of California, Berkeley

November 19, 1973

* M.S. Thesis

DISPERSION OF GASEOUS EMISSIONS FROM A GROUND-LEVEL LINE SOURCE

Kirk D. Winges, Edward A. Grens II, and Theodore Vermeulen

ABSTRACT

The spread of vehicular pollutants from along a freeway can be modeled by a family of cross-sectional planes, usually taken perpendicular to the freeway axis. When calculations in such a plane are carried out using a finite-element grid, the emission source can be represented as one, or several, of the two-dimensional grid elements.

Relations between velocity and turbulent transport are redeveloped here from conventional equations for conservation of momentum and of matter. Three elementary cases are considered, in this initial step toward future comprehensive analysis of freeway configurations by a continuity method: parallel flow over a uniform plane; flow over a discontinuity in surface roughness; and, most significant for the freeway problem, flow over a perpendicular barrier attached to a uniform plane.

The velocity profiles used for these respective cases were based, first, on both logarithmic and power-law models; second, on data from Plate[6]; and third, on wind-tunnel data from Nagabhushaniah[42]. In the barrier-flow case, the pressure field was estimated by assuming potential, or inviscid, flow. In all three cases, the turbulent transport was characterized by an eddy viscosity for momentum transfer and by an eddy diffusivity for mass transfer, which were set equal and were calculated by the momentum equations.

Concentration profiles were computed in each case for the region downwind from a ground-level emission source. These calculations demonstrate the feasibility of predicting concentration profiles by the continuity method, in configurations for which the velocity and pressure profiles are known or predictable.

TABLE OF CONTENTS

LIST OF FIGURES

I. INTRODUCTION

The problem of small-scale atmospheric dispersion, which has received extensive recent attention in relation to air pollution, actually has been of long standing concern to meteorologists. In principle the question is this: For a given ground-level emission source, how does one predict the spread of the contaminant? This problem has been pursued from a broad spectrum of approaches and has yielded an immense volume of literature. However, very few researchers have studied microscale dispersion in the range of ten to one hundred feet.

From the standpoint both of health hazards and of the photochemical smog-forming reactions, dispersion effects near the emission source may be highly significant. Therefore, the present study considers the spread of pollutants in the vicinity of a ground-level emission source, the immediate objective being concentration plots at distances within a few hundred feet from the source. The complexity of this problem in terms of the multiplicity of contributing factors precludes the hope for general solutions in analytic form. Indeed previous characterizations of the lower layers of the atmosphere have always been approximations derived from, at best, semi-empirical theories.

In specific cases, such as air flow around freeways, the basic flow direction is set upby large-scale atmospheric effects. On the local scale this is modified first by the local geometry, including ground roughness. In some cases such local effects can completely change the general direction, as in the situation called channeling in which air is constrained to flow lengthwise in valleys or between buildings.

These local geometric effects are in turn modified by local thermal conditions - either large-scale as with local atmospheric stability, or small-scale as by differential ground heating set up by differing absorptions of solar energy. Finally, for the scale that is of interest here, a perturbation such as the turbulence generated by automobiles becomes important.

The path toward being able to treat more complex situations can be defined by first solving highly simplified cases. The techniques used here are based as much as possible on theoretical principles. The transport of contaminants can be attributed to two mechanisms, convection and diffusion. For averaged equations, even in the small scale treated here, molecular diffusion can only be significant in a very shallow layer close to the ground (the viscous sub-layer), which is sufficiently thin to be neglected in most treatments. Convection then is the only mechanism considered, but a convection highly complicated by the presence of turbulent fluctuations in the velocity and concentration. These fluctuations can be modeled using an effective, or "eddy", diffusivity, so the equations still represent a diffusion process. Hereafter, unless specified otherwise, diffusion will refer to eddy diffusion.

Despite the presence of fluctuations, the mean values of the velocity and concentration are the most significant influence on the spread of emissions. Both the magnitude and direction of the velocity vector are strongly dependent on the nature of the surface. The absence of data for other systems has restricted our treatment to three cases: flow over a flat plate of uniform roughness, flow over a flat plate with a discontinuity in roughness, and flow over a barrier set perpendicular to a flat plate. Although dispersion

in the first case has been treated previously by Roberts and others,[1] dispersion in the last two cases has not received previous attention. The last two cases, referred to as disturbed boundary layers, are the focus of this research. Characterization of the velocity profiles for flow over these geometries has been accomplished from available data. An approximation to the pressure gradient has also been derived.

In order to calculate the dispersion of a pollutant emitted in these flow geometries, we utilize the equation for conservation of mass. In order to solve this equation, further simplification is needed. Here it has been assumed that no thermal effects are involved. Also no consideration has been given to additional sources of turbulence. We have developed an equation representing the conservation of momentum for these systems, which together with the empirical velocities and approximated pressures is solved for the turbulent flux of momentum. The mass-momentum transfer analogy then states that the mechanism for turbulent mass and momentum transfer must be the same, hence the flux of mass (in this case characterized by eddy diffusivity) can be calculated. Together with the empirical velocities, the eddy diffusivities are used in the mass-conservation equation to calculate contrations of a contaminant emitted from a point source in a two-dimensional flow geometry.

The solutions thus obtained suffer from two defects: inaccuracies in the assumptions, and inaccuracies in the data. The limiting features of the present solutions are the input velocity data and the pressure-term approximation. However, although no concentration data are available for verification, it is believed that the solutions indicate a reasonable picture of the processes involved. Future studies will hopefully in-

clude data for verification - either for these or other flow geometries - as the technique is applicable to any system for which sufficient velocity and pressure data are available.

II. MATHEMATICAL BACKGROUND

ENSEMBLE AVERAGING

Approaches to handle the turbulent characteristics of atmospheric flows differ primarily in the assumptions and approximations employed; however, virtually all approaches use some form of averaging. From the practical standpoint the use of time- and space-averages is very convenient, but in theoretical calculations time- and space-averages lead to unavoidable difficulties.[2] As a result we use ensemble averaging for our treatment; that is, the average of values of all tests that could be run under identical conditions. In laminar flow, variables measured under identical conditions would always yield identical values, to within experimental error. In turbulent flow this is not the case owing to the random behavior of the system variables; however, for any given set of conditions, the averages of any sufficiently large set of measurments all should be the same. To use these averages the Reynolds conditions represented in Eqs. 1-5 are applied. Here an overbar indicates an ensemble average of the expression beneath it, and f and g are any variables.

$$\overline{f + g} = \overline{f} + \overline{g} \tag{1}$$

$$\overline{af} = a\overline{f} \quad \text{if } a = \text{constant} \tag{2}$$

$$\overline{a} = a \quad \text{if } a = \text{constant} \tag{3}$$

$$\overline{\frac{\partial f}{\partial s}} = \frac{\partial \overline{f}}{\partial s} \quad \text{where } s = x, y, \text{ etc.} \tag{4}$$

$$\overline{\overline{f} \cdot \overline{g}} = \overline{f} \cdot \overline{g} \tag{5}$$

Instantaneous variables will generally be divided into

two components, the mean (ensemble average) value, and a fluctuation from this mean value, denoted by a prime.

$$f = \overline{f} + f'$$

We note that since $\overline{f'} = 0$, then

$$\overline{fg} = \overline{f}\cdot\overline{g} + \overline{f'g'} + \overline{\overline{f}g'} + \overline{\overline{g}f'}$$
$$\overline{fg} = \overline{f}\cdot\overline{g} + \overline{f'g'} \qquad (6)$$

In the treatment of the following equations, both sides of the expression are averaged, after which Eqs. 1-6 are used to separate out individual variables.

Mass Conservation

The equation for mass conservation in a fluid flow, the continuity equation, is:[3]

$$\frac{\partial \rho}{\partial t} + \mathrm{div}(\rho\vec{u}) = 0 \qquad (7)$$

Here $\vec{u}$ is the vector velocity, ρ is the density, and t is time. Since we are considering incompressible flow (low Mach number), and neglecting thermal effects, we assume ρ is constant, and Eq. 7 can be written as:

$$\mathrm{div}(\vec{u}) = 0 \qquad (8)$$

or

$$\frac{\partial u}{\partial x} + \frac{\partial v}{\partial y} + \frac{\partial w}{\partial z} = 0 \qquad (9)$$

Here u, v, and w are the x, y, and z components of the velocity respectively. Now, averaging Eq. 9 with the use of the Reynolds conditions, Eqs. 1 and 4, we have

$$\frac{\partial \overline{u}}{\partial x} + \frac{\partial \overline{v}}{\partial y} + \frac{\partial \overline{w}}{\partial z} = 0 \qquad (10)$$

Since we are concerned with dispersion problems, the mass conservation of a particular species in a multi-component mixture is also of interest. With no chemical reaction, the mass-balance equation for a component A is given as:[4]

$$\frac{\partial C_A}{\partial t} + \text{div}(\vec{u}C_A) = D_A \cdot \text{div grad}(C_A) \qquad (11)$$

Here C_A is the concentration of A, and D_A is its molecular diffusivity. Taking the averages of both sides of Eq. 11 and using Eqs. 1, 4, and 6, we have:

$$\frac{\partial \overline{C}_A}{\partial t} + \frac{\partial \overline{uC}_A}{\partial x} + \frac{\partial \overline{vC}_A}{\partial y} + \frac{\partial \overline{wC}_A}{\partial z} + \frac{\partial \overline{u'C_A'}}{\partial x} + \frac{\partial \overline{v'C_A'}}{\partial y} + \frac{\partial \overline{w'C_A'}}{\partial z}$$
$$= D_A \cdot \left(\frac{\partial^2 \overline{C}_A}{\partial x^2} + \frac{\partial^2 \overline{C}_A}{\partial y^2} + \frac{\partial^2 \overline{C}_A}{\partial z^2}\right) \qquad (12)$$

Momentum Conservation

The law of momentum conservation in terms of the Navier-Stokes stress formulation is generally written as:[5]

$$\rho\frac{\partial \vec{u}}{\partial t} + \rho\vec{u}\cdot\text{grad}(\vec{u}) - \vec{F} + \text{grad}(P) - \text{div}\mu(\text{grad}\ \vec{u}$$
$$+ (\text{grad}\ \vec{u})^*) - \text{grad}(\lambda\ \text{div}\ \vec{u}) = 0 \qquad (13)$$

In this expression $\vec{F}$ is any external body force (such as gravity), P is the pressure, μ and λ are the first and second viscosity coefficients, and the asterisk refers to the transpose of the matrix inside its parentheses. Div $\vec{u}$ is much smaller than def $\vec{u}$ (the term multiplying μ), hence the term involving the second viscosity coefficient is neglected, and, again, the

density is assumed constant. Taking averages, in component form we have:

$$\rho\frac{\partial\bar{u}}{\partial t} + \rho\left(\bar{u}\frac{\partial\bar{u}}{\partial x} + \bar{v}\frac{\partial\bar{u}}{\partial y} + \bar{w}\frac{\partial\bar{u}}{\partial z}\right) + \rho\left(\frac{\partial\overline{u'^2}}{\partial x} + \frac{\partial\overline{u'v'}}{\partial y} + \frac{\partial\overline{u'w'}}{\partial z}\right) - \bar{f}_x + \frac{\partial\bar{P}}{\partial x} - \mu\left(\frac{\partial^2\bar{u}}{\partial x^2} + \frac{\partial^2\bar{u}}{\partial y^2} + \frac{\partial^2\bar{u}}{\partial z^2}\right) = 0 \quad (14)$$

$$\rho\frac{\partial\bar{v}}{\partial t} + \rho\left(\bar{u}\frac{\partial\bar{v}}{\partial x} + \bar{v}\frac{\partial\bar{v}}{\partial y} + \bar{w}\frac{\partial\bar{v}}{\partial z}\right) + \rho\left(\frac{\partial\overline{u'v'}}{\partial x} + \frac{\partial\overline{v'^2}}{\partial y} + \frac{\partial\overline{v'w'}}{\partial z}\right) - \bar{f}_y + \frac{\partial\bar{P}}{\partial y} - \mu\left(\frac{\partial^2\bar{v}}{\partial x^2} + \frac{\partial^2\bar{v}}{\partial y^2} + \frac{\partial^2\bar{v}}{\partial z^2}\right) = 0 \quad (15)$$

$$\rho\frac{\partial\bar{w}}{\partial t} + \rho\left(\bar{u}\frac{\partial\bar{w}}{\partial x} + \bar{v}\frac{\partial\bar{w}}{\partial y} + \bar{w}\frac{\partial\bar{w}}{\partial z}\right) + \rho\left(\frac{\partial\overline{u'w'}}{\partial x} + \frac{\partial\overline{v'w'}}{\partial y} + \frac{\partial\overline{w'^2}}{\partial z}\right) - \bar{f}_z + \frac{\partial\bar{P}}{\partial z} - \mu\left(\frac{\partial^2\bar{w}}{\partial x^2} + \frac{\partial^2\bar{w}}{\partial y^2} + \frac{\partial^2\bar{w}}{\partial z^2}\right) = 0 \quad (16)$$

Application of these equations to the geometries considered requires inputs - most significantly velocities. Discussion of these velocities begins with large-scale atmospheric flows.

GENERAL ATMOSPHERIC MOTION

Large-scale atmospheric-pressure variation and atmospheric motion are set up by the earth's rotation and by differential solar heating of the surface. The equations are rotational in nature, and contain centrifugal and Coriolis terms. For the outer layers of the atmosphere, approximate solutions are available neglecting the shear-stress gradients.[6] One such solution gives prevailing values of the geostrophic wind components effective at the top of the atmospheric boundary layer.[7] Inside the boundary layer, the shear stresses modify substantially the geostrophic wind vector, rottating it to the left in the northern hemisphere.

The surface boundary layer itself has two regions. The outer region exhibits the effects of the pressure gradient, the Coriolis force, and the shear stress. Close to the ground there exists another layer in which the structure of the flow field is determined solely by the flux of momentum to the ground, and this is the layer of interest in the present study. Momentum flux to the ground is strongly influenced, along with the depth of this layer, by the specific nature of the surface (expressed as a drag coefficient).[8] Combination of the data of Swinbank[9] for the atmosphere with that of Klebanoff[10] for flow over a flat plate shows this layer to be about 150 meters deep. Within this vertical distance, the momentum flux to the ground can be regarded as the dominant factor in determining the velocity profile. Flow over a uniform flat plate serves as a starting point for calculations in this layer.

FLOW OVER A UNIFORM FLAT PLATE

The equation of motion for flow in one direction (here, the x-direction) over an infinite flat plate (parallel to the x-axis), simplified from Eq. 14, is

$$\frac{\partial \overline{u}}{\partial t} + \frac{\partial \overline{u'^2}}{\partial x} + \frac{\partial \overline{u'v'}}{\partial y} + \frac{\partial \overline{u'w'}}{\partial z} + \frac{1}{\rho}\frac{\partial \overline{P}}{\partial x} - \overline{f}_x - \nu\left(\frac{\partial^2 \overline{u}}{\partial x^2} + \frac{\partial^2 \overline{u}}{\partial y^2} + \frac{\partial^2 \overline{u}}{\partial z^2}\right) = 0 \quad (17)$$

where:

$$\nu = \frac{\mu}{\rho} \quad (18)$$

For steady state, zero pressure gradient, and no body force, $\overline{u}$ is a function of z only, and this equation becomes

$$\nu\frac{\partial^2\overline{u}}{\partial z^2} - \frac{\partial\overline{u'w'}}{\partial z} = 0 \qquad (19)$$

or

$$\rho\nu\frac{\partial\overline{u}}{\partial z} - \rho\overline{u'w'} = \text{constant} = \tau_o \qquad (20)$$

In the last expression τ_o has units of a shear stress, hence τ_o is called the shear stress at the ground. Since only kinematic characteristics of the flow are involved, τ_o only affects the velocity profile through the combination τ_o/ρ, which has the units of a velocity squared. Therefore, a friction velocity, u^*, is defined as $(\tau_o/\rho)^{\frac{1}{2}}$. Dimensional considerations then show that only the parameters u^* and ν can influence the flow.

From these considerations Prandtl's universal law of the wall is derived.[11] For this law the surface or wall is considered smooth in the sense that the mean height of surface protrusions is less than the friction length, $z^* = \nu/u^*$. This is almost never the case in the atmosphere, and as a result the height and spacing of the protrusions do have a large influence in the region close to the wall. However, for heights considerably greater than the friction length, it appears that neither the viscosity nor the local surface properties influence the slope of the velocity profile.[12] The velocity derivative in this region is determined solely by the parameter u^* and the height. This allows the description of velocity differences, whereas the actual velocity scale must be specified separately.

Convective Transport

1. The Logarithmic Profile

It is immediately possible to form the combination

u^*/z, which has the dimensions of a velocity gradient. Let

$$\frac{\partial u}{\partial z} = \frac{1}{k}\frac{u^*}{z} \tag{21}$$

Here k is a universal constant, known as von Karman's constant, lying in the general range of 0.2 to 0.8 and usually set at 0.4.[13] Integration yields:

$$\frac{\bar{u}}{u^*} = \frac{1}{k}\ln(z) + C \tag{22}$$

or more commonly,

$$\frac{\bar{u}}{u^*} = \frac{1}{k}\ln\left(\frac{z}{z_o}\right) \tag{23}$$

Here C or z_o is a function of the surface conditions and establishes the scale of the velocity profile at its lower limit of validity; z_o is called the roughness parameter. Detailed derivations are given by von Karman[14] and Prandtl.[15] The range of validity for Eq. 23, called the logarithmic layer, is the atmospheric region of interest in this study. The logarithmic relation can also be deduced from the considerations of the previous section my matching the flows of the inner and outer regions of the atmospheric boundary layer.[16]

Quite frequently one needs to displace the flow above some plane, for example, a region of vegatation of a uniform height. In this case a zero-plane displacement can be introduced to establish the start of the logarithmic profile. This is incorperated as:

$$\frac{\bar{u}}{u^*} = \frac{1}{k}\ln\left(\frac{z - d_o}{z_o}\right) \tag{24}$$

Here d_o is the zero-plane displacement introduced by Rosby and Montgomery.[17] The controlling parameter, u^*, enters through the top boundary condition. Unfortunately it is not directly measurable at this point, when the lower boundary layer is treated separately from the planetary boundary. Perhaps the best method would be direct measurement of the shear stress at the wall. This involves building an apparatus for each site, which is not desirable. Consequently, usually it is determined by measurement of $\bar{u}$ at some height, z, and back calculation of u^*, with z_o known or assumed. z_o is a function of the ground roughness; typical values, given by Blackadar,[18] are listed in Table 1. All methods of determining u^* in the atmosphere show that its value normally lies between 10 and 100 cm/sec.[19] With $\nu = 0.15$ cm^2/sec for normal air, the friction length, ν/u^*, ranges from 0.0015 to 0.015 cm. Thus it is evident that almost all ground surfaces on earth have protrusions larger than the friction length, and hence must be considered rough.

2. The Power-Law Profile

Depending on the nature and needs of a problem, we might also describe the velocity profile by a power-law distribution of the form:

$$\frac{\bar{u}}{u_1} = \left(\frac{z}{z_1}\right)^p \qquad (25)$$

The subscript 1 here refers to a measured value at some height; and p is a parameter, presumably independent of height, determined by at least one more measured velocity at a different height. Although the power law does not have a dimensional property

akin to Eq. 21 for the logarithmic law, DeMarris[20], in a comparison of the two laws asserted that for a wide variety of conditions the two predicted profiles are quite similar, but the power law is superior for use in a wider range of meteorological conditions. Literature values for p range from 0.13[21] to 0.28.[22] Neither law can be used for situations where the condition of uniformity of the surface is relaxed.

When large-scale changes in the surface conditions are involved, large separations usually occur, and multidimensional flow is encountered. It is to this area that the major effort of this research is addressed.

Non-Convective Transport

1. Plume-Based Models

For material transport in the lower atmosphere, with emissions from a point source, the primary transport is by convection, not molecular diffusion; therefore the molecular diffusion terms in Eq. 12 are usually dropped. We consider only steady-state flow in one direction, for which Eq. 12 is written as:

$$\bar{u}\frac{\partial \bar{C}_A}{\partial x} + \frac{\partial \overline{u'C'_A}}{\partial x} + \frac{\partial \overline{v'C'_A}}{\partial y} + \frac{\partial \overline{w'C'_A}}{\partial z} = 0 \qquad (26)$$

The unaccounted-for terms involving the fluctuation velocities remain. Richardson[23] viewed these terms as behaving like a molecular diffusivity. That is, he postulated that the fluctuation terms were given by a mean concentration gradient multiplied by a new transport coefficient called the eddy diffusivity. The following equations represent Richardson's assumptions.

$$\overline{u'C_A'} = -K_x \frac{\partial \overline{C}_A}{\partial x} \tag{27}$$

$$\overline{v'C_A'} = -K_y \frac{\partial \overline{C}_A}{\partial y} \tag{28}$$

$$\overline{w'C_A'} = -K_z \frac{\partial \overline{C}_A}{\partial z} \tag{29}$$

Here K_x, K_y, and K_z are the eddy diffusivities in the x, y, and z directions. Substitution of these terms into Eq. 26 gives the form:

$$\overline{u}\frac{\partial \overline{C}_A}{\partial x} = \frac{\partial}{\partial x}(K_x \frac{\partial \overline{C}_A}{\partial x}) + \frac{\partial}{\partial y}(K_y \frac{\partial \overline{C}_A}{\partial y}) + \frac{\partial}{\partial z}(K_z \frac{\partial \overline{C}_A}{\partial z}) \tag{30}$$

In order to solve this equation, assumptions must be made concerning the eddy diffusivities. Frequently, one treats the case of an instantaneous point source, and assumes both the velocities and eddy diffusivities are constant with respect to z. The equation is then written in the Lagrangian framework, that is by incorperation of the motion due to the mean velocity convection into a time derivative:

$$\frac{\partial \overline{C}_A}{\partial t} = K_x \frac{\partial^2 \overline{C}_A}{\partial x^2} + K_y \frac{\partial^2 \overline{C}_A}{\partial y^2} + K_z \frac{\partial^2 \overline{C}_A}{\partial z^2} \tag{31}$$

The solution for an instantaneous point source of strength Q is then:

$$\frac{\overline{C}_A}{Q} = (4\pi t)^{\frac{3}{2}}(K_x K_y K_z)^{-\frac{1}{2}} \exp\left(\frac{-1}{4t}\left(\frac{x^2}{K_x} + \frac{y^2}{K_y} + \frac{z^2}{K_z}\right)\right) \tag{32}$$

The basic Gaussian nature of this and related solutions has led many researchers to model atmospheric dispersion by the well known Gaussian plume. In this representation instantaneous point source emissions, or puffs, are considered to be convected downstream at a constant velocity and to spread in all directions

with a Gaussian shape. Usually some relation is formulated between the downstream distance and the standard deviation of the concentration. This technique is usually reserved for elevated sources such as stacks, however, many researchers have used it for ground-level emission sources as well. Johnson, Ludwig, Dabbert, and Allen[24] used the relation:

$$\sigma_z = ax^b \qquad (33)$$

with σ_z as the standard deviation. The a and b were constants which could be varied with atmospheric stability.

Shair and Drivas[25] compared the use of such Gaussian plume models both with their own data and with the predictions of more sophisticated solutions to be discussed later. Their results show that the Gaussian plume model does not give satisfactory results, and that far greater accuracy can be obtained by more exact techniques. The difficulties with the plume models lie in the assumptions of constant wind and eddy diffusivity. In particular, Shair and Drivas showed that the center of the puff is not convected downstream at a constant rate, but in fact increases in velocity with downstream distance. The assumption of constant eddy diffusivity, as will be shown later, is not consistent with a non-uniform velocity. For use in describing small scale diffusion near the ground, plume-based models do not yield the accuracy desired.

2. Eddy Diffusivity Models

Two basic avenues are being followed today for describing the diffusive spread of emissions: the gradient transport approach, and the statistical

approach. The present research is concerned mainly with the gradient transport approach, which yields to theoretical calculations more conveniently. Inherent in the gradient transport treatment is the postulation of eddy diffusivities to account for turbulent terms in the transport equations. The neglect of thermal conditions and external sources of turbulence allows the assumption of isotropy of eddy diffusivity; that is, $K_x = K_y = K_z = K$. The basic technique is to relax the assumptions of constant wind and eddy diffusivity, and thereby to find specific solutions to Eq. 30. The mass/momentum analogy can be used to arrive at assumptions regarding the eddy diffusivity. It is used here by simply stating that the mechanism for non-convective transport of momentum must be the same as that for non-convective transport of mass. More specifically, just as an eddy diffusivity is postulated for the transfer of a gas component, an eddy viscosity is postulated for the transfer of momentum from the upper layers of the atmosphere downward.

Eq. 19 reflects the assumption that the net velocity (horizontal and x-directed) varies only with z. It is also assumed that the protrusions on the surface are sufficiently large that throughout the entire region the effect of molecular viscosity is negligible with respect to the effect of the fluctuating velocities. Now we set

$$\overline{u'w'} = -K_\nu \frac{\partial \bar{u}}{\partial z} \tag{34}$$

where K_ν is the eddy viscosity in the z direction. Combination with Eq. 19 gives:

$$K_\nu \frac{\partial^2 \bar{u}}{\partial z^2} + \frac{\partial K_\nu}{\partial z} \frac{\partial \bar{u}}{\partial z} = 0 \tag{35}$$

If $\bar{u}$ has the form of Eq. 23 corresponding to the logarithmic velocity profile, Eq. 35 becomes

$$-K_\nu \frac{u^*1}{k}\frac{1}{z^2} + \frac{\partial K_\nu}{\partial z}\frac{u^*1}{k}\frac{1}{z} = 0 \qquad (36)$$

$$\frac{\partial K_\nu}{K_\nu} = \frac{\partial z}{z} \qquad (37)$$

$$K_\nu \propto z \qquad (38)$$

By analogy to this behavior of eddy viscosity, it is also assumed that the eddy diffusivity is proportional to z. Hence,

$$K = K_1 z \qquad (39)$$

where K_1 is a proportionality constant. This result was used by Prandtl[26] in the mixing-length theory. The diffusion equation that then must be solved is:

$$\left(\frac{u^*}{k}\ln\left(\frac{z}{z_o}\right)\right)\frac{\partial \bar{C}_A}{\partial x} = K_1 z\frac{\partial \bar{C}_A}{\partial x} + K_1 z\frac{\partial \bar{C}_A}{\partial y} + K_1 z\frac{\partial \bar{C}_A}{\partial z} + K_1\frac{\partial \bar{C}_A}{\partial z} \qquad (40)$$

No general analytic solution is available for this equation, but it may be solved numerically with the proper boundary conditions.

Similarly, adoption of the power-law model, Eq. 25, for the atmospheric velocity profile gives another correlation for K.

$$K_\nu \frac{u_1}{z_1^p} p(p-1) z^{(p-2)} + \frac{\partial K_\nu}{\partial z}\frac{u_1}{z_1^p} p z^{(p-1)} = 0 \qquad (41)$$

$$\frac{\partial K_\nu}{K_\nu} = (1-p)\frac{\partial z}{z} \qquad (42)$$

$$K_\nu \propto z^{(1-p)} \tag{43}$$

Using the analogy again, we find:

$$K = K_1 z^{(1-p)} \tag{44}$$

which yields the diffusion equation:

$$u_1 \left(\frac{z}{z_1}\right)^p \frac{\partial \overline{C}_A}{\partial x} = K_1 z^{(1-p)} \frac{\partial^2 \overline{C}_A}{\partial x^2} + K_1 z^{(1-p)} \frac{\partial^2 \overline{C}_A}{\partial y^2} + K_1 z^{(1-p)} \frac{\partial^2 \overline{C}_A}{\partial z^2} + K_1 z^{-p} \frac{\partial \overline{C}_A}{\partial z} \tag{45}$$

Eq. 45 also requires numerical techniques for solution; however, various steps have been taken toward approximate solutions. Roberts, in an unpublished paper summarized by Sutton[28] and also by Calder[29], neglected the y- and x-second derivatives. (The neglect of the x-derivative was validated by Walters.[30]) The resulting solution is:

$$\overline{C}_A = \frac{Q(2p+1)}{\Gamma\left(\frac{p+1}{2p+1}\right)\frac{u_1}{z_1^p}} \left(\frac{u_1/z_1^p}{K_1(2p+1)^2 x}\right)^{\frac{p+1}{2p+1}} \exp\left(\frac{-u_1 z^{(2p+1)}}{K_1(2p+1)^2 x z_1^p}\right) \tag{46}$$

for a continuous ground-level source of strength Q. Here Γ is the gamma function, or generalized factorial. A plot of the two-dimensional concentration grid for Eq. 46 with Q = 1 and p = 1/7 is shown in Fig. 1.

The condition of ground-level emission restricts application of this equation in freeway diffusion problems to distances well downstream of the source. A low-mixing zone close to the ground slows the upward movement of contaminants beyond what would be expected in normal freeway situations. Even in freeway situations the actual source is always somewhat elevated, and

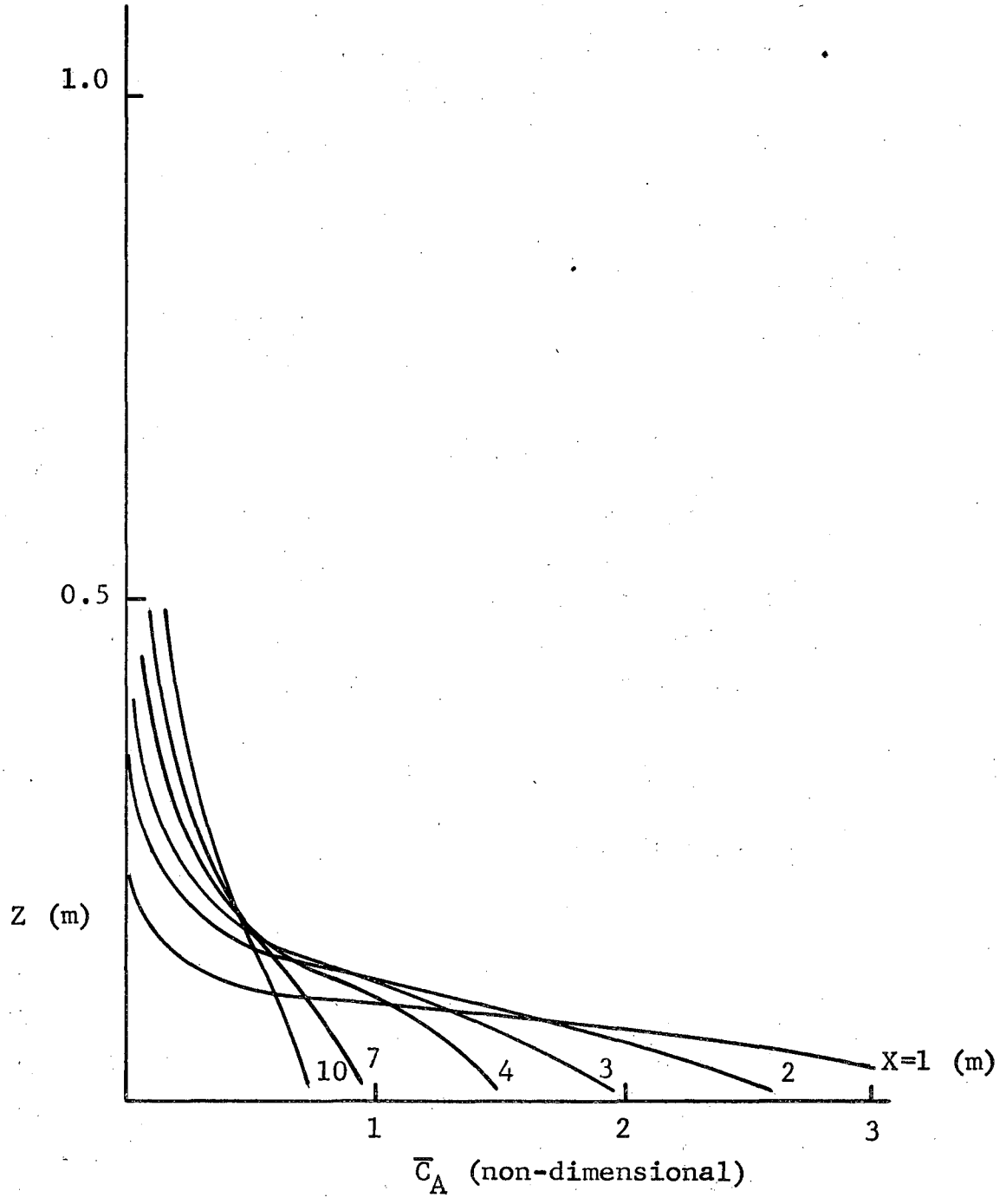

Fig. 1: Concentration Profiles Downstream of a Ground-Level Emission Source, Plotted from Eq. 46

this zone does not need to be completely traversed.

Eqs. 40 and 45 have also been applied to the case of an instantaneous point source by addition of a term containing the time gradient of concentration. Theoretical analysis of Eq. 40 by Chatwin[31], using the method of moments, involves a coordinate transformation in which an apparent velocity at which the puffs are carried downstream is postulated. He found this velocity to be:

$$u_a = \frac{u^*}{k} \ln\left(\frac{K_1 e^{-\gamma t}}{z_o}\right) \qquad (47)$$

where γ Euler's constant and u_a is the apparent velocity. His results also showed the standard deviation for the concentration values at the ground to be proportional to the time after emission. Saffman[32] generalized Eq. 45 by assuming the power of proportionality with height for the eddy diffusivity to be an ajustable parameter.

$$K \propto z^c \qquad (48)$$

His results show:

$$u_a \propto t^{\left(\frac{p}{2-c}\right)} \qquad (49)$$

$$\sigma_x \propto t^{\left(1+\frac{p}{2-c}\right)} \qquad (50)$$

for the ground-level values of the concentration.

Shair and Drivas[33] compared the two results with their data and showed better agreement for the generalized case of Saffman; however, this may be primarily due to the use of the additional parameter in Saffman's technique. Better agreement is almost certainly expected for the power-law model as it contains an additional degree of freedom; however, the

available data are not sufficient to conclude that the power law is a better description of the atmospheric profile. The instantaneous point-source emission case is, however, a good point for comparison of the two profiles. Further study involving more exact experiments should resolve the question of which velocity equation is more sound for diffusion analysis, but since flexibility to describe differing atmospheric conditions is not necessary for the present treatment, either profile should be applicable.

NON-UNIFORM FLOW

Flow Over a Discontinuity in Surface Roughness

Extention of the ideas developed for the uniform flat plate case to that of disturbed atmospheric boundary layers begins with the simplest case; a step change in the roughness of a flat plate. Previous work has treated only the aerodynamic characteristics of this problem. Data useful for atmospheric applications were obtained by Sterns and Lettau[34], and also, particularly, Bradley.[35] These data indicate that within the atmospheric boundary layer, a new boundary layer forms slightly ahead of the discontinuity. This is called an internal boundary layer, and the entire flow is sometimes referred to as internal-boundary-layer flow. Downstream of the discontinuity one sees close to the ground a shear layer whose properties are governed by the local ground conditions, and above the internal boundary layer thickness a region controlled by the upstream ground conditions, with a blending region in between. The equations describing this flow, two-dimensional in nature, and based on simplified versions of Eqs. 10, 14, and

16, are:

$$\frac{\partial \overline{u}}{\partial x} + \frac{\partial \overline{w}}{\partial z} = 0 \tag{51}$$

$$\overline{u}\frac{\partial \overline{u}}{\partial x} + \overline{w}\frac{\partial \overline{u}}{\partial z} + \frac{\partial \overline{u'^2}}{\partial x} + \frac{\partial \overline{u'w'}}{\partial z} + \frac{1}{\rho}\frac{\partial \overline{P}}{\partial x} = 0 \tag{52}$$

$$\overline{u}\frac{\partial \overline{w}}{\partial x} + \overline{w}\frac{\partial \overline{w}}{\partial z} + \frac{\partial \overline{u'w'}}{\partial x} + \frac{\partial \overline{w'^2}}{\partial z} + \frac{1}{\rho}\frac{\partial \overline{P}}{\partial z} = 0 \tag{53}$$

To simplify these equations further, the normal turbulent stresses ($\overline{u'^2}$ and $\overline{w'^2}$) are incorperated into the pressure gradient, and the term is subsequently neglected.[36] This permits dropping Eq. 53 and re-writting Eq. 52 in the form:[37]

$$\overline{u}\frac{\partial \overline{u}}{\partial x} + \overline{w}\frac{\partial \overline{u}}{\partial z} + \frac{\partial \overline{u'w'}}{\partial z} = 0 \tag{54}$$

Elliot[38] and later Plate and Hidy[39] used a technique based on the Karman-Pohlhausen method of integration of the equations of motion to arrive at approximate solutions to Eqs. 51 and 54. This technique involved introducing a logarithmic velocity profile and integrating Eq. 54 to obtain solutions for the internal-boundary-layer thickness and the shear stress at the surface. (The shear stress here is considered a function of x only, but is discontinuous at the internal-boundary-layer thickness.) Their results, which involve complicated empirical polynomials and simultaneous solution of nonlinear equations, are as follows:

$$\frac{k^2 x}{z_{o2}} = \frac{\delta}{z_{o2}}\frac{N}{P} \tag{55a}$$

$$\frac{\overline{u}_2}{u_2^*} = \frac{1}{k}\ln\left(\frac{z}{z_{o2}}\right) \tag{55b}$$

$$u_2^{*2} = u_1^{*2}\left(\frac{P}{D} + 1\right) \tag{55c}$$

$$D = c^4 + c^3(b-1) + c^2 \tag{55d}$$

$$P = 2bc^3 + c^2(3b^2-2b) + c(b^3-b^2) - b^2 \tag{55e}$$

$$N = c^4 b + c^3(2b^2-4b) + c^2(b^3-6b^2+2b) - 2cb^3 + 2b^2 \tag{55f}$$

$$c = \ln\left(\frac{\delta}{z_{o2}}\right) \tag{55g}$$

$$b = \ln\left(\frac{z_{o2}}{z_{o1}}\right) \tag{55h}$$

Here δ is the internal-boundary-layer thickness, z_{o1} and z_{o2} are the roughness parameters for the two regions, u_1^* and u_2^* are the friction velocities for the two regions, and D, P, and N are the empirical polynomials. The technique for applying this system is to first calculate b by Eq. 55h and then solve Eqs. 55a, 55e, 55f, and 55g simultaneously for c and δ. These quanities are then used in Eqs. 55b, 55c, and 55d to calculate $\overline{u}_2$, the velocity in the region downstream of the discontinuity and below the internal-boundary-layer thickness. The velocity not in this region is assumed to be unchanged from its upstream value; that is, the logarithmic law with z_{o1} as the roughness parameter and u_1^* as the friction velocity.

Efforts by Panofsky and Townsend[40] to eliminate the shear-stress discontinuity have involved modifying the assumed velocity profile so as to have an additional blending property (the difficulties of this are discussed by Taylor[41]). The values calculated using these modifications do not differ greatly from those of Eqs. 55a-h. It is believed that the equations presented represent an accurate description of the

flow situation. Velocities calculated by Eqs. 55a-h are used in the present study.

Flow Over a Barrier

We next consider the flow in which the boundary layer is disturbed by the placement of barriers. The simplest case is that of a vertical wall or fence of infinite extent in the y-direction, and finite extent in the z-direction, placed in contact with the surface boundary (this case is also called "shelterbelt" flow). Very little theoretical study has been made of this case; most results have evolved from data analysis. Nagabhushaniah[42] studied flow over this geometry in a wind tunnel. Velocities measured by him at various points around the fence are the primary data used in the present study. Two free-stream velocities and several fence heights were used in his study. From this and other data, Plate[43] identifies seven regions in the flow field, which are displayed in Fig. 2 reproduced from Plate. The most significant of these regions is the formation of a region of recirculation, or cavity, behind the fence. The flow as characterized by Plate is quite akin to that of a free shear layer in which a segment of air with velocity U_∞ is set next to a stationary body of air, a situation which has been solved by Görtler.[44] For this simplified case the assumption of an eddy viscosity is again made:

$$\overline{u'w'} = K_\nu \frac{\partial \bar{u}}{\partial z} \tag{56}$$

Here K_ν is a function of x only and is given as:

$$K_\nu = \frac{xU_\infty}{4\varphi} \tag{57}$$

1, Undisturbed boundary layer (outer layer)
2, Region of hill influence (middle layer)
3, Region of reestablishing boundary layer (inner layer)
4, Blending region between middle and outer layer
5, Blending region between inner and middle layer
6, Standing eddy zone
7, Potential outer flow

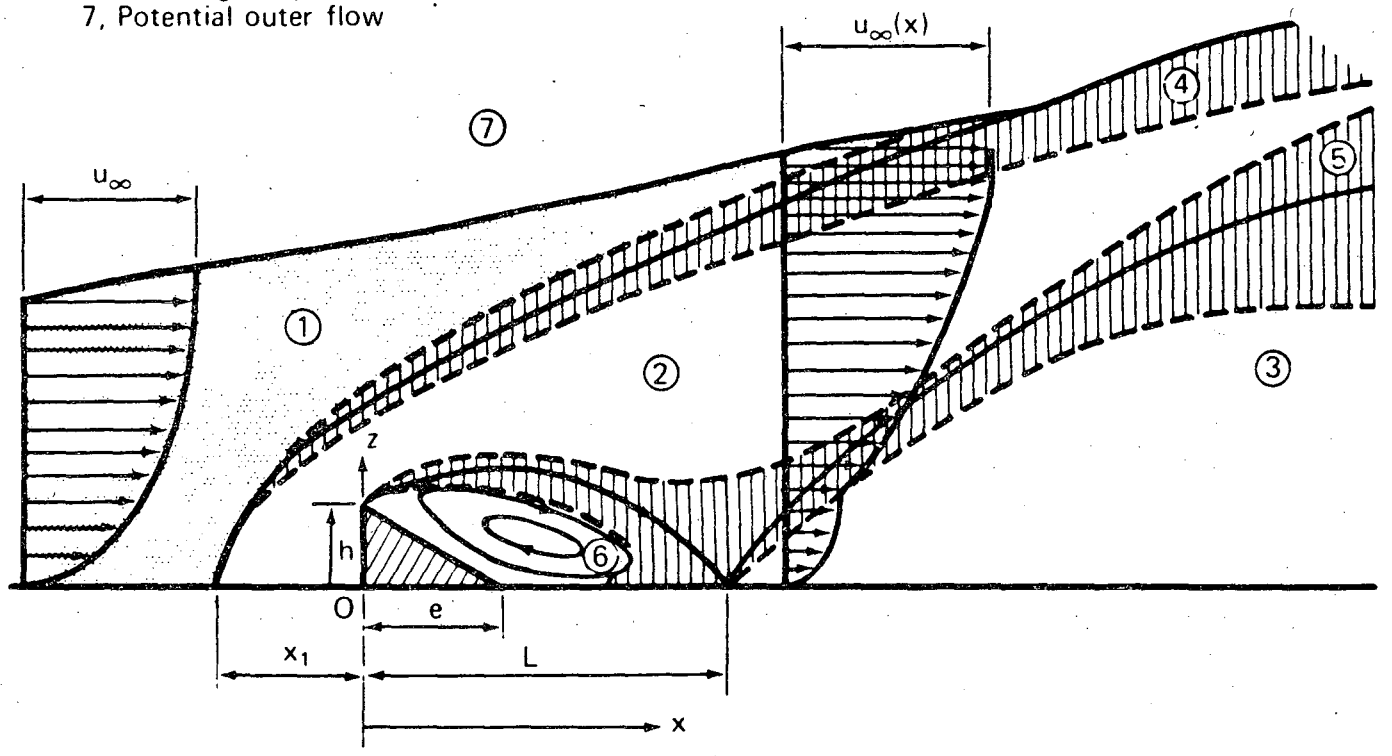

Fig. 2: Plate's Identification of the Flow Regions for Barrier Flow

where φ is an empirically determined constant. The velocity is then solved as:

$$\overline{u} = \frac{U_\infty}{2}(1-\text{erf}(\xi)) \tag{58}$$

$$\text{erf}(\xi) = \frac{2}{\sqrt{\pi}}\int_0^\xi e^{-m^2}dm \tag{59}$$

$$\xi = \frac{\varphi(z-z_r(x))}{x} \tag{60}$$

The displacement of the z coordinate by $z_r(x)$ is caused by the presence of the ground. In the pure free-shear-layer flow, the center of the layer is constant at the height of the barrier, but when the horizontal surface is included, the center of the layer is drawn down. As a result, $z_r(x)$ is a reference point which Plate has taken to be the height at which

$$\frac{\overline{u}}{U_\infty} = \frac{1}{2} \tag{61}$$

Plate also compares the data of Chang[45] with the model, and concludes that good agreement is obtained owing partly to the empirical constant, φ. Further analysis leads to the prediction of Gaussian-shaped shear-stress profiles which agree well with Chang's data, and deviate only in areas where $(z-z_r)/x$ is negative. That the data are well fitted by the free-shear-layer solution is not surprising in view of the physical similarity; however, the usefulness of these results for diffusion study must still be questioned. The accuracy of the equations in predicting velocity profiles for the barrier case is not clear. Although Plate aserts that good agreement is obtained for the data of Chang, the data of Nagabhushaniah do not agree. As a result the error-func-

tion solution is not used to characterize the velocity profiles in this study.

Finally, brief mention should be made of diffusion near buildings, which has been studied principally by Halitsky.[46] The flow equations for a three-dimensional object are complicated beyond the capabilities of current techniques; however, experimental data exist for such situations.[47] The hope in this and other related research is that freeway-diffusion situations can be calibrated or even fully modeled by consideration of the few data and simplified analyses available.

III. NUMERICAL ANALYSIS FOR SIMPLE GEOMETRIES

This investigation has been aimed mainly at establishing techniques for predicting dispersion rates in disturbed atmospheric boundary layers. General solutions for these problems are precarious, because their inherant simplifications involve the risk of making them inapplicable to real situations. As a result empirical modeling and numerical solution have been used in developing techniques for calculating dispersion rates in a few simplified flow situations. Specificly, what is calculated are concentration profiles resulting from ground-level emission sources. The simplified flow geometries treated allow restriction of this investigation to two-dimensional flow. The source, actually a line source perpendicular to the plane of consideration, can be treated as a point source.

For two idealized flows, flow over a flat plate with a discontinuity in surface roughness, and flow over a barrier set perpendicular to a flat plate, the same calculational technique is used. First, empirical models for the velocity profiles are established; then an approximation to the pressure field is derived from analysis of potential flow in these geometries. These results are both used in the momentum-conservation equation to calculate eddy diffusivity profiles. The diffusivities, combined with the velocity profiles, are then used in the steady-state conservation-of-mass equation to calculate the concentration profiles produced by a continuous line source.

The usefulness of the solution technique is established by application to the uniform flat plate case and comparison of the results obtained with the

solution of Roberts, presented in Fig. 1. Calculations carried out for the uniform-flat-plate case include treatment of both velocity profiles developed previously: the logarithmic profile, Eq. 23, and the power-law profile, Eq. 25. In addition, since the solution of Roberts neglects horizontal diffusion, and since the current technique does not, we test this assumption by calculating a similar numerical solution, neglecting horizontal diffusion. This solution establishes that neglect of horizontal diffusion produces almost no error in our calculated values of the concentration.

The analysis of disturbed boundary layers (discontinuity in roughness and flow over a barrier cases) consists of applying the described technique to ground-level emission sources located in these geometries. For the discontinuity-in-roughness case, the velocity profiles of Plate and Hidy (Eq. 55a-h) are used. For the barrier-flow case the velocity profiles are a characterization of the data of Nagabhushaniah. All calculations of concentration profiles have been carried out for typical values of the input parameters, and are presented as illustrations of the technique.

We begin with the simplest case of flow over a uniform flat plate.

UNIFORM-FLAT-PLATE CASE

Tracer dispersion, or pollutant spread from a ground source, in the uniform-flat-plate case is considered here using the two boundary-layer velocity profiles previously discussed: the logarithmic law (Eq. 23), and the power law (Eq. 25). Eq. 12, usable with these models, describes the conservation of mass

for an identifiable component whose physical properties are not different from the rest of the fluid. Such a component is referred to as a "passive admixture".

From Eqs. 12 and 25 with the assumption of a steady-state, and gradient transport by means of an eddy diffusivity only, Eq. 30 was developed for dispersion from a point source in the atmosphere. The solution presented in Fig. 1 incorperated the additional assumptions of a power-law velocity profile, a continuous line source of infinite y-extent, absence of horizontal diffusion, and ground-level emission.

Eqs. 34-44 demonstrate how specification of the velocity profile enables the mass/momentum transfer analogy to establish the diffusivity. However, specifying the source to be ground-level leads to unrealistically slow dispersion because of the presence of a weakly-mixed layer near the ground. Since in any freeway situation the source is always somewhat elevated, close to the source inaccurate predictions of concentration values would normally be calculated. To increase the accuracy of prediction, the present analysis treats the source as a uniformly mixed region of finite x- and z-extent and infinite y-extent.

The present technique treats both velocity functions and investigates the validity of neglecting horizontal dispersion. If we assume isotropy of eddy diffusivity, Eq. 30 becomes:

$$\overline{u}\frac{\partial \overline{C}_A}{\partial x} = \frac{\partial}{\partial x}\left(K\frac{\partial \overline{C}_A}{\partial x}\right) + \frac{\partial}{\partial z}\left(K\frac{\partial \overline{C}_A}{\partial z}\right) \qquad (62)$$

For this flow the eddy diffusivity is a function of z only, thus:

$$\overline{u}\frac{\partial \overline{C}_A}{\partial x} = K\frac{\partial^2 \overline{C}_A}{\partial x^2} + K\frac{\partial^2 \overline{C}_A}{\partial z^2} + \frac{\partial K}{\partial z}\frac{\partial \overline{C}_A}{\partial z} \qquad (63)$$

Because this partial differential equation is elliptic, not parabolic as are many atmospheric diffusion equations, it requires boundary conditions enclosing its domain. These are to be given at the surface, and infinitely far from the source in each of the other directions.

These requirements are not surprising, as in any urban enviornment the concentrations at distances far from a source do not drop to zero, but approach finite background levels. Supporting evidence from Shair and Drivas[48], and Ranzieri[49], concerning carbon monoxide, indicate that concentrations imeasurably different from background levels are attained a few hundred feet downstream from typical sources. The boundary conditions for Eq. 63 are then:

$$\frac{\partial \overline{C}_A}{\partial x} \to 0 \quad \text{as} \quad x \to \infty \qquad (64)$$

$$\frac{\partial \overline{C}_A}{\partial z} \to 0 \quad \text{as} \quad z \to \infty \qquad (65)$$

$$\frac{\partial \overline{C}_A}{\partial x} \to 0 \quad \text{as} \quad x \to -\infty \qquad (66)$$

$$\frac{\partial \overline{C}_A}{\partial z} = 0 \quad x > \frac{x_e}{2},\ x < -\frac{x_e}{2},\ z = 0 \qquad (67)$$

$$\overline{C}_A = Q \quad \text{for} \quad -\frac{x_e}{2} < x < \frac{x_e}{2},\ 0 < z < z_e \qquad (68)$$

The final condition describes the source as a uniformly mixed region within a z-interval, z_e, called the emission height, and an x-interval, x_e, called the emission length.

Eq. 63 was solved for both logarithmic and power-law velocity profiles (and their respective eddy-dif-

fusivity profiles) by means of iterative finite-difference calculations. A complete discussion of the solution technique is presented in Appendix 1. The results for typical values of the input parameters are shown in Fig. 3 for the logarithmic profile, and Fig. 4 for the power-law profile. The input values, outlined below, match as closely as possible those used in plotting Eq. 46.

Logarithmic Law

Surface Roughness	0.01m
Velocity Condition	$\bar{u}$=5m/sec @ z=10m
Proportionality Constant for Eddy Diffusivity with height	0.1m/sec
Emission Strength	1.0
Emission Height	0.1m
Emission Length	0.5m

Power Law

Exponent, p	0.17
Velocity Condition	$\bar{u}$=5m/sec @ z=10m
Proportionality Constant for Eddy Diffusivity with Height	$0.1m^{2-p}$/sec
Emission Strength	1.0
Emission Height	0.1m
Emission Length	0.5m

Inspection of Figs. 3 and 4 indicates first that there is very little difference between the results arising from the two profiles. Comparison with Fig. 1 indicates the effect of using an emission source of finite height. Downstream the two solutions agree in form quite well, while upstream the mixed region of the emission-height treatment tends to dominate the shape of the concentration profiles.

To establish that these differences originated in the emission-height treatment of the source, and were not due to neglect of horizontal diffusion employed for Fig. 1, a numerical solution using the emission-height treatment but also ignoring horizontal

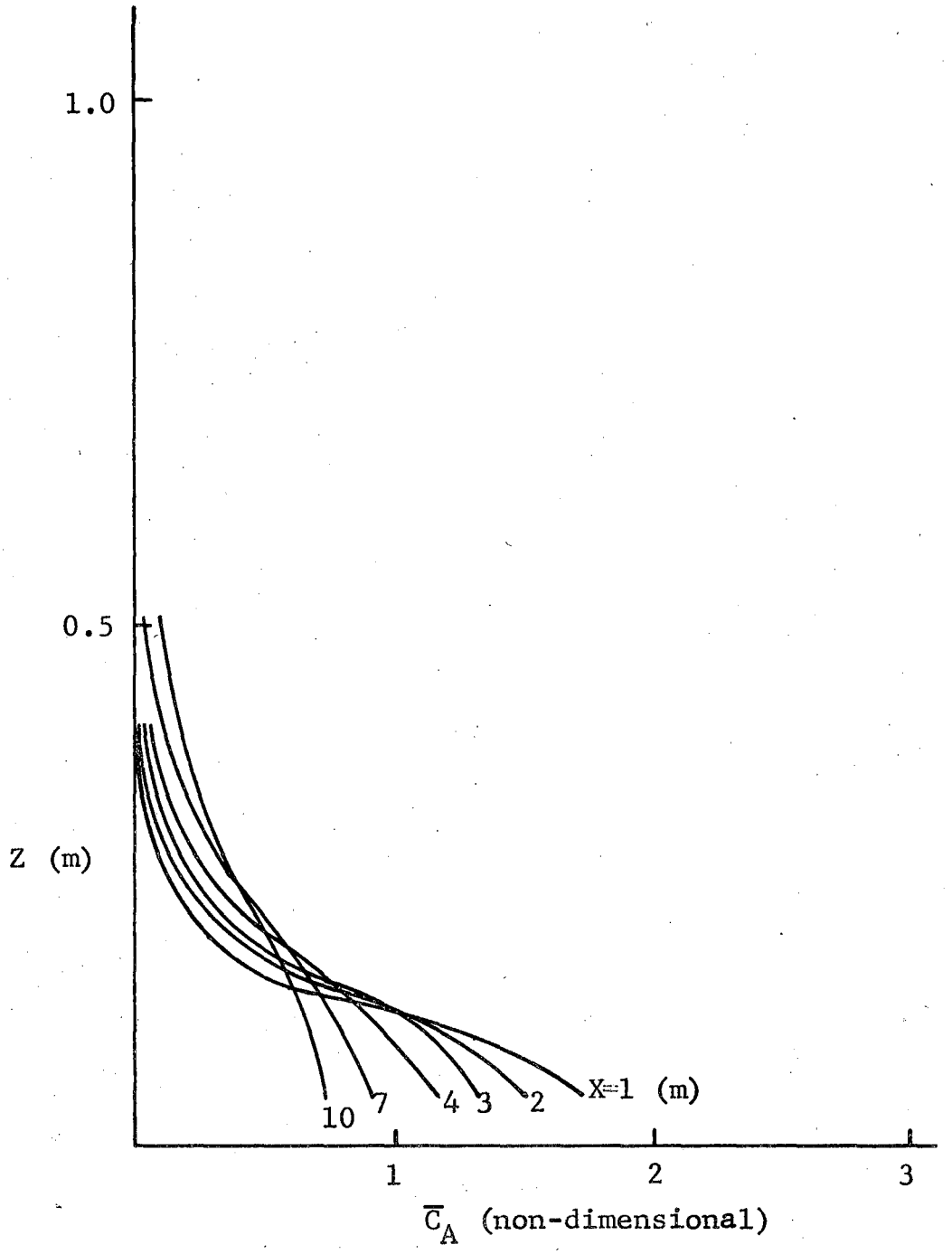

Fig. 3: Concentration Profiles Downstream of a Ground-Level Emission Source, for Flow Over a Uniform-Flat-Plate, Using the Logarithmic Velocity Profile

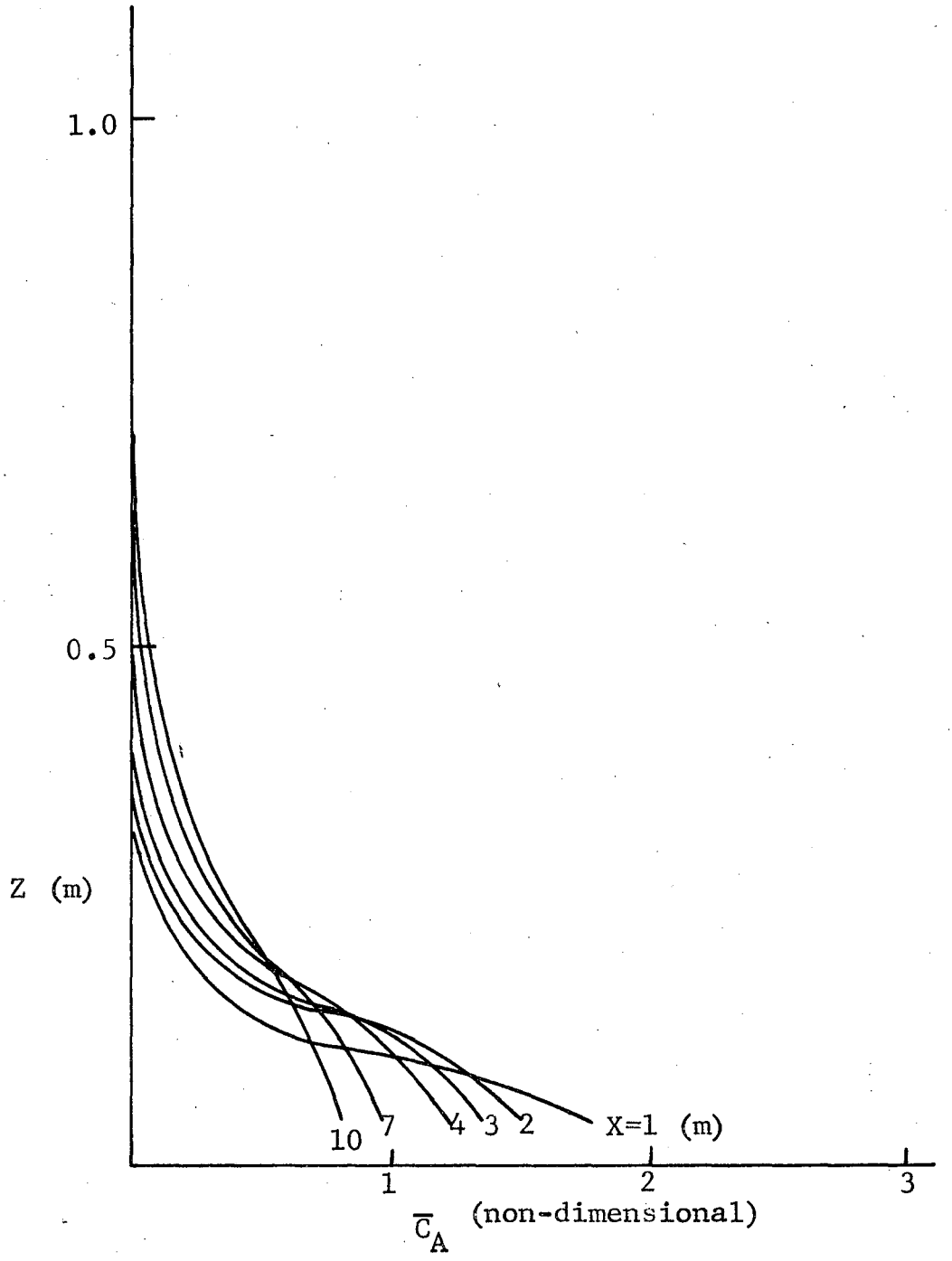

Fig. 4: Concentration Profiles Downstream of a Ground-Level Emission Source, for Flow Over a Uniform-Flat Plate, Using the Power-Law Profile to Describe the Velocity

diffusion was obtained for the logarithmic-law velocity profile. Eq. 63, modified by the neglect of horizontal diffusion, becomes:

$$\bar{u}\frac{\partial \bar{C}_A}{\partial x} = K\frac{\partial^2 \bar{C}_A}{\partial z^2} + \frac{\partial K}{\partial z}\frac{\partial \bar{C}_A}{\partial z} \qquad (69)$$

Matching inputs were again used in this equation and solution was obtained numerically and plotted in Fig. 5. As can be seen from Figs. 3 and 5, neglect of horizontal diffusion introduces almost no difference for these systems. It is seen, however, that the difference between Fig 1 and Figs. 3 and 4 are not due to the form of equation assumed. Eq. 46, used in plotting Fig. 1, and Fig. 5 were both presented as solutions to the same differential equation, Eq. 69. The similarity of Fig. 5 to Figs. 3 and 4 indicates that Fig. 1 differs from the other three because of the differences in the emission height formulation.

It is also seen that for the uniform-flat-plate case, the parabolic treatment is quite acceptable; however, later cases involving disturbed atmospheric boundary layers may not allow neglect of the horizontal-diffusion term. As a result we will find the development of these elliptic-solution techniques useful.

The good agreement between solutions calculated using the logarithmic- and power-law velocity equations may in part be due to the selection of constants for the illustration to give closely matching profiles. However, since constants are to be selected for the idalized cases studied here, the question of which profile to use as a background description of the velocity in disturbed atmospheric boundary layers is not crucial in this study. Although more diverse atmospheric conditions are described by the power-law profile, they are not involved in this study.

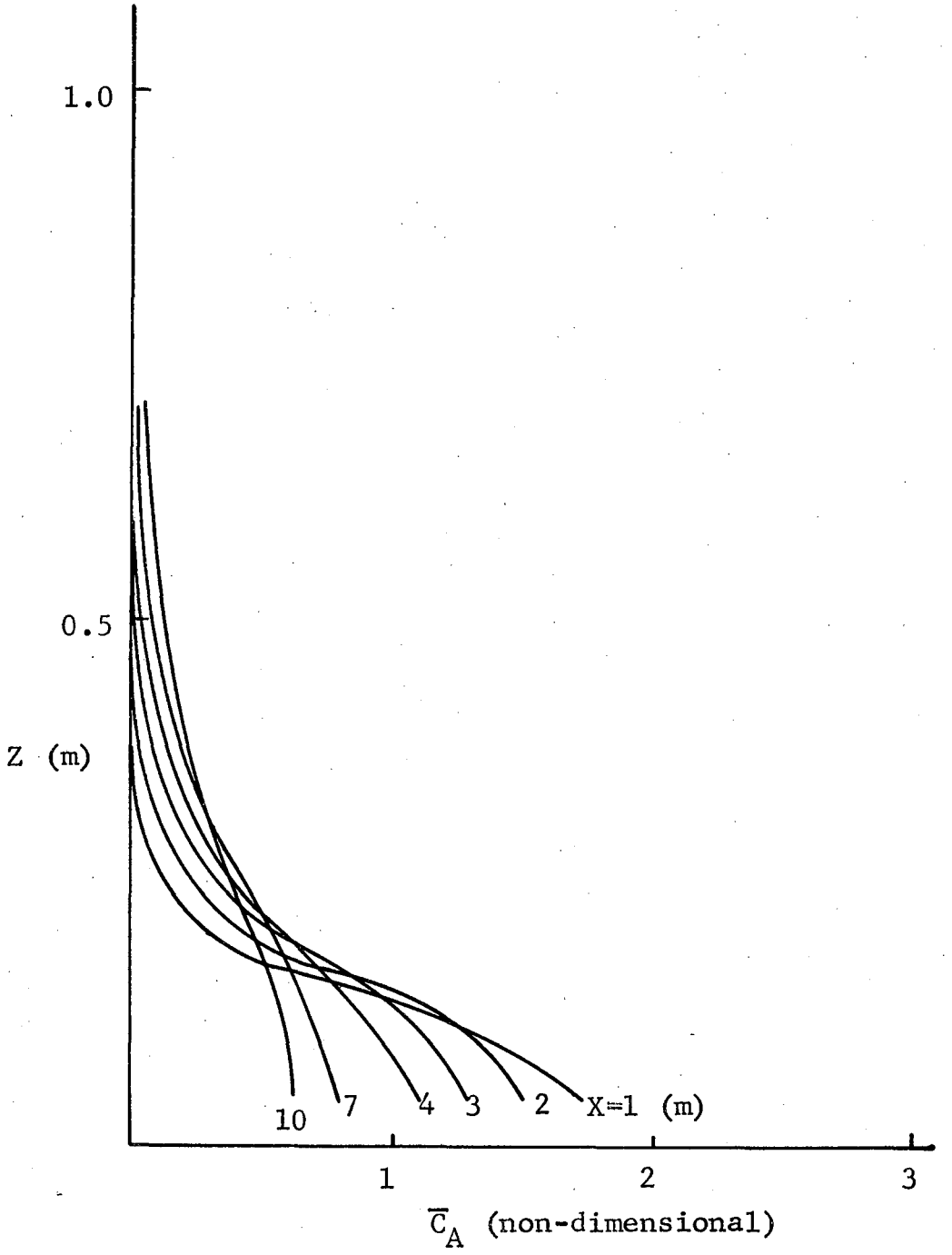

Fig. 5: Concentration Profiles Downstream of a Ground-Level Line Source, for Flow Over a Uniform-Flat Plate, Using a Logarithmic Velocity Profile, Solved by a Parabolic Treatment of the Equations Involved (Neglect of Horizontal Diffusion)

Since previous work in the discontinuity flow has used the logarithmic law as a background velocity, it has been adopted for the present treatment of this case. However, since the wind-tunnel study of Nagabhushaniah reported a power-law background velocity, we use the power law as our background velocity for consideration of flow over a barrier.

FLOW OVER A DISCONTINUITY IN SURFACE ROUGHNESS

The flow situation involved when a discontinuity in surface roughness is encountered is depicted in Fig. 6. For the logarithmic velocity profile, the roughness parameter, z_o, becomes the factor that controls the profile shape. In the case of a step change in the value of this parameter, adjustment of the flow occurs over a considerable region downstream. Upstream of the discontinuity, the flow is characterized by a roughness parameter, z_{o1}. Close to the discontinuity, an internal boundary layer forms which continues to grow, until far downstream the flow is characterized by the downstream roughness parameter, z_{o2}.

Elliot[50] and Plate and Hidy[51] treated the aerodynamic characteristics of this problem, and developed Eqs. 55a-h to give the velocity profiles downstream of the discontinuity. An averaging technique is used to establish the velocity in the region around the discontinuity, and the results are plotted in Fig. 7.

We now wish to use these velocities in the momentum conservation equation to establish eddy diffusivities. Eqs. 52 and 53 were derived to express momentum conservation for this flow. Since the potential flow solution for this case differs only slightly from uniform flow, we follow the ideas of Plate[52]

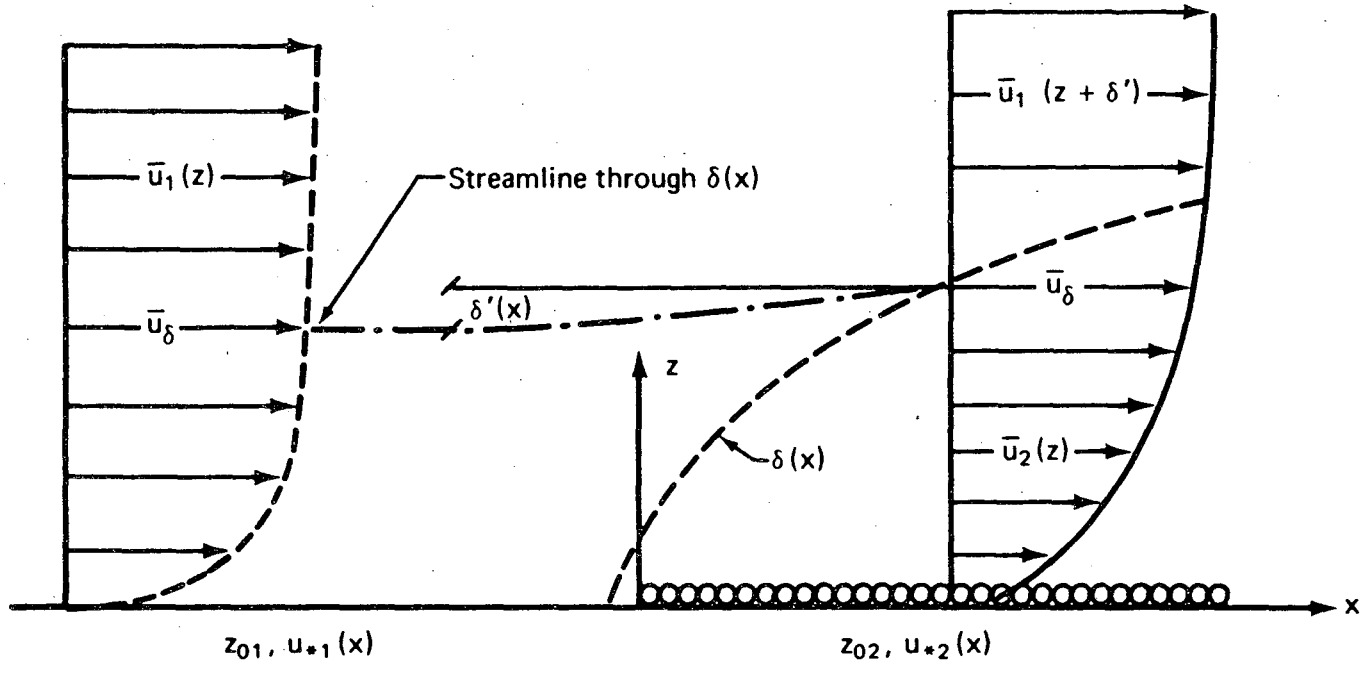

Fig 6: Flow Over a Discontinuity in Surface Roughness Parameter

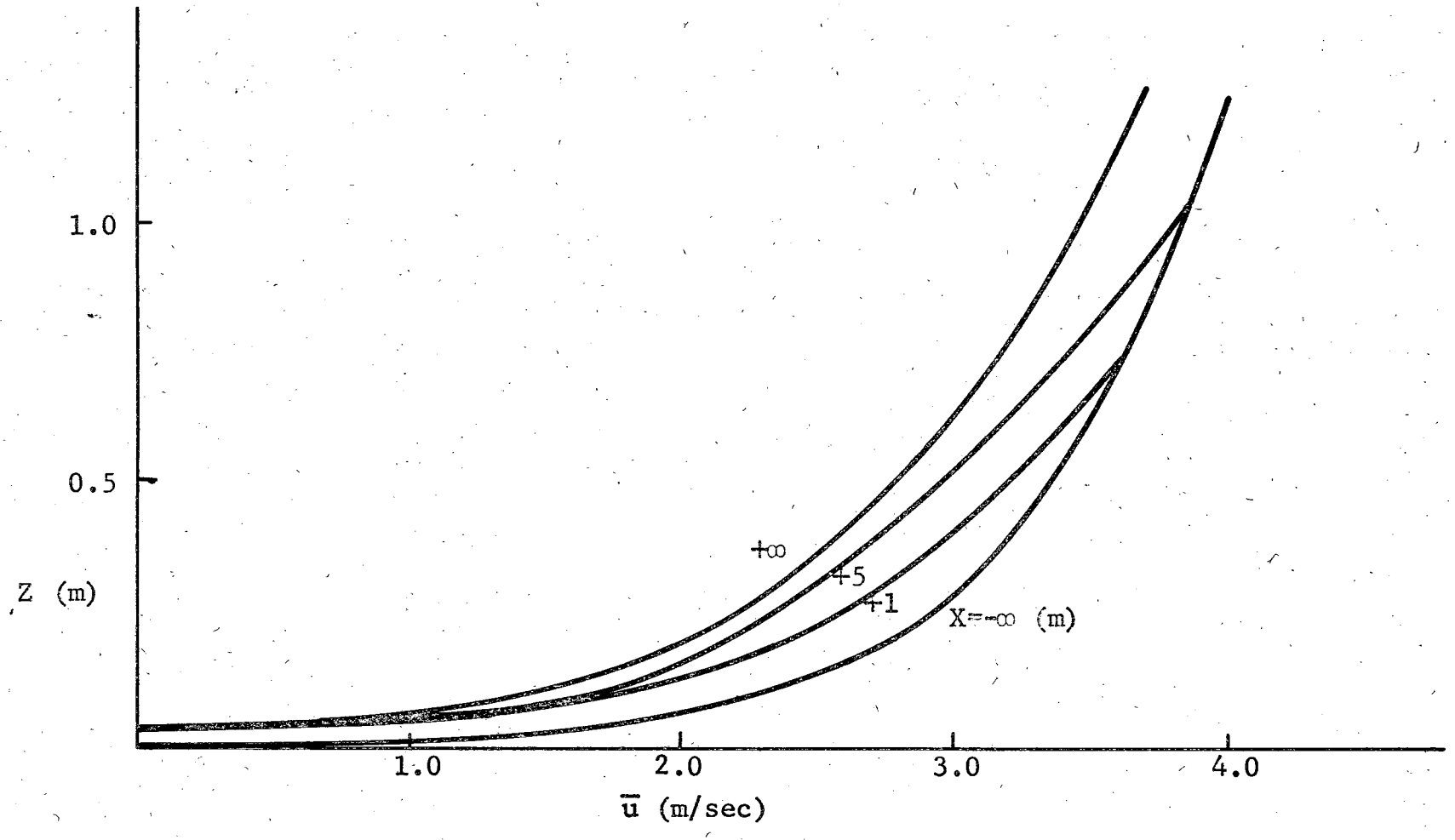

Fig. 7: Velocity Profiles for Flow Over a Discontinuity in Surface Roughness Parameter

and incorperate the normal turbulent stresses, $\overline{u'^2}$ and $\overline{w'^2}$, into the pressure terms and then neglect the pressure terms. This allows the development of Eq. 54 to describe the momentum conservation. Analogous to the logarithmic-law behavior, we assume that the eddy viscosity (and hence the eddy diffusivity) is proportional to height, but here the proportionality constant is a function of x.

$$K_\nu = K = z \cdot K_1(x) \tag{70}$$

Remembering the definition of the friction velocity as equal to $(\tau_o/\rho)^{\frac{1}{2}}$, and combining Eqs. 20, 34, and 70 with neglect of laminar viscosity, we arrive at

$$u^{*2} = \rho K_1(x) z \frac{\partial \bar{u}}{\partial z} \tag{71}$$

Now, using the relation for the velocity given by Eq. 55b, we find:

$$K_1 = k u_2^* \tag{72}$$

with u_2^* expressed as a function of x by Eq. 55c. This gives the eddy diffusivity field as $K = k u_2^* \cdot z$, shown in Fig. 8.

Using these solutions in the convective-diffusion equation, we are able to compute concentrations produced by emission sources located near such discontinuities in roughness. The equation of interest is developed from Eq. 12 by neglecting molecular diffusion, assuming steady state, considering only the two-dimensional problem (that is, ignoring all y-derivatives), and using a gradient-transport formulation with isotropic eddy diffusivity, to yield:

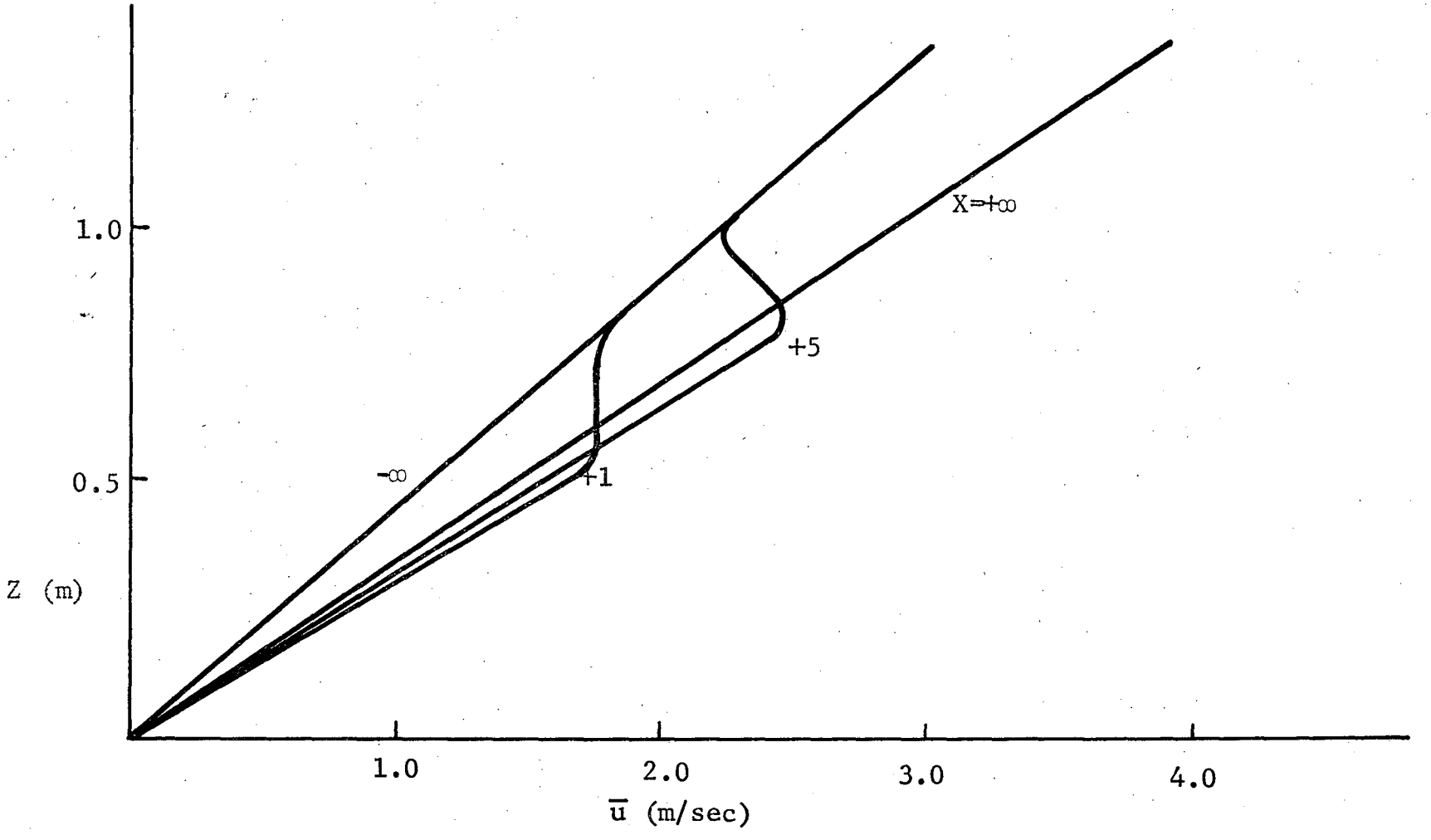

Fig. 8: Diffusivity Profiles for Flow Over a Discontinuity in Surface Roughness Parameter

$$\overline{u}\frac{\partial \overline{C}_A}{\partial x} + \overline{w}\frac{\partial \overline{C}_A}{\partial z} = \frac{\partial}{\partial x}\left(K\frac{\partial \overline{C}_A}{\partial x}\right) + \frac{\partial}{\partial z}\left(K\frac{\partial \overline{C}_A}{\partial z}\right) \qquad (73)$$

The vertical velocities needed for this equation are calculated from the two-dimensional continuity equation, simplified from Eq. 10:

$$\frac{\partial \overline{u}}{\partial x} = -\frac{\partial \overline{w}}{\partial z} \qquad (74)$$

A typical solution is presented in Fig. 9, with upstream and far-downstream conditions matching the logarithmic law. A complete discussion of the solution technique can be found in Appendix 2. In this illustration the discontinuity is an increase in the surface roughness, and the source is located a short distance upstream of the discontinuity. However, the technique is applicable to any arrangement.

Inspection of Fig. 9 indicates an increase in the vertical distribution of the contaminant as the stream passes over the discontinuity. This upward transport is due in part to the general increase in dispersion caused by higher roughness on the downstream side of the discontinuity. However, as seen in Fig. 8, the eddy diffusivity at any constant height is higher in the blending region than at points further upstream or downstream. This indicates the presence of a shear layer around $\delta(x)$. This shear layer causes an additional upward movement of contaminants apart from that caused by the larger roughness on the downstream side.

A source for inaccuracy in this treatment is the input values of the velocity. Although it is not clear to what extent the inaccuracies in this treatment are due to data inaccuracies and to what extent they are due to invalid assumptions, it seems reasonable that more accurate velocity determination will inevidably lead to better prediction of downstream

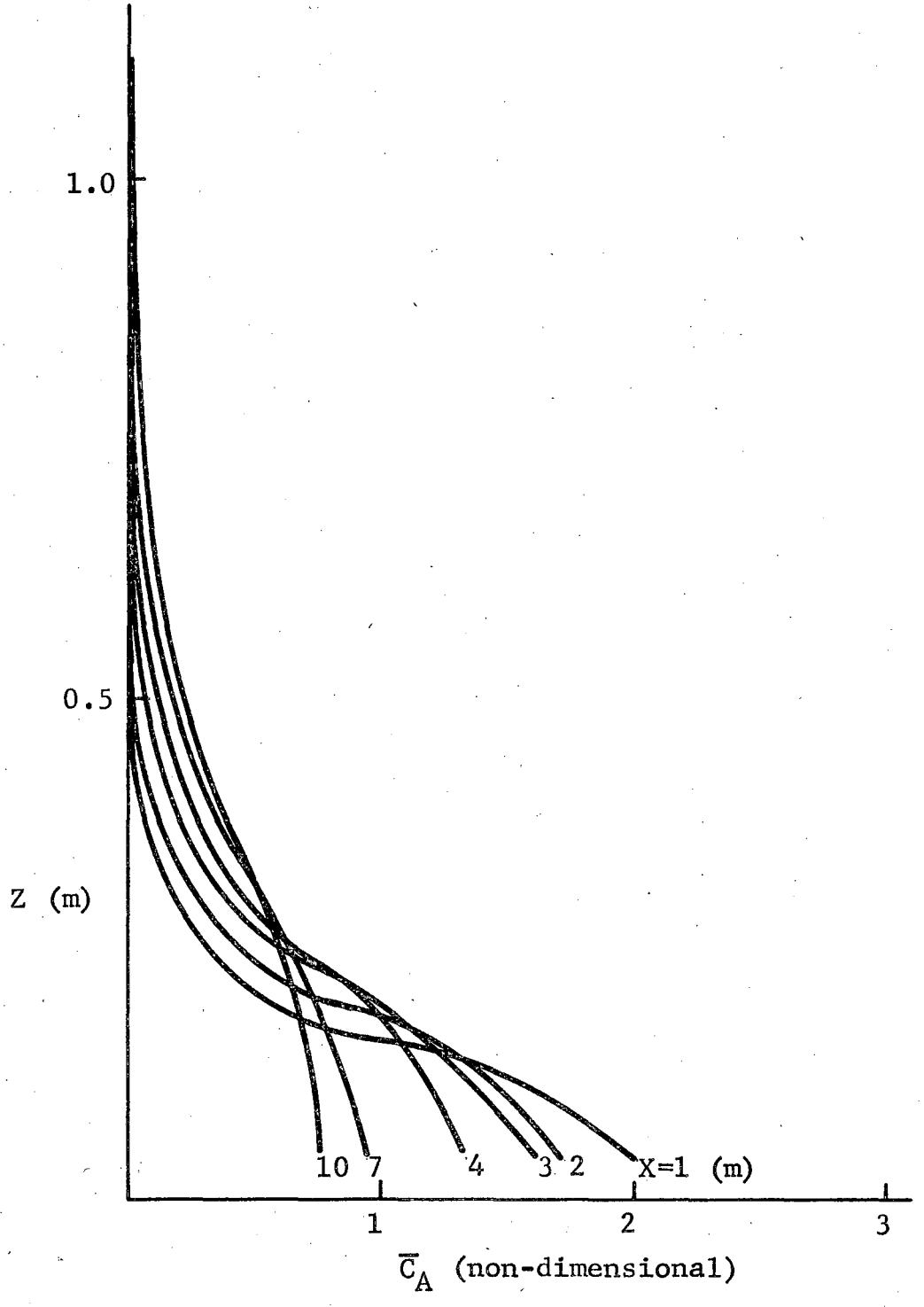

Fig. 9: Concentration Profiles Downstream of a Ground-Level Emission Source, for Flow Over a Discontinuity in Surface Roughness Parameter

concentration values.

FLOW OVER A PERPENDICULAR BARRIER

Fig. 2 depicts the geometry for flow over a perpendicular barrier, also referred to as "shelterbelt" flow. This case was selected as the prototype for all ground-connected obstacles to wind flow. Far upstream and downstream of the barrier, the flow is an undisturbed atmospheric boundary layer described by the power-law velocity profile. The presence of a solid barrier establishes pressure gradients which in turn result in separation of the flow, beginning slightly ahead of the barrier and continuing downstream for about twelve times the height of the barrier as measured by Nagabhushaniah.[53] Since this separated region, or cavity, is in contact with the outer flow through turbulent fluctuations only, not through convection, the outer flow is deflected around the separation streamline, or cavity boundary. This deflection causes modification of the local velocity vector, as well as increased turbulence in the region above and downstream of the cavity.

Diffusion in this flow has not received previous attention. The previous workers have been concerned only with the aerodynamic characteristics of the flow. In particular, Plate has used a modification of the free-shear layer flow solved by Görtler[44] to describe his velocity profiles. Eqs. 58-60 represent Plate's solution. We find this solution to be unapplicable for the present study. The background power-law profiles observed in the atmosphere (and those used in related wind-tunnel studies) are generally very curved close to the ground, and very flat away from the ground. For any barrier of

reasonable size, the value of the background velocity measured at a height equivalent to the barrier height would not be greatly different from that measured at a height several times the barrier height; indeed this is the case in the wind tunnel study of Nagabhushaniah. In order for continuity of the air flow to be maintained, the total rate of air flow through each vertical plane, x=constant, must be the same. This means that the air which is deflected around the cavity must be added to the relatively flat profile in the region above the cavity, with a clear possibility of producing values of the velocity near the cavity that are larger than those at much greater heights. A maximum in the velocity profile occurs frequently in the data of Nagabhushaniah, but is not allowed for in the error-function solution used by Plate. Thus the solution of Plate cannot be made to adhere to the continuity relation for cases of interest.

Plate in deriving his solution assumed the eddy viscosity to be a function of x only. Even in the undisturbed boundary layer, the eddy viscosity is a function of height. Certainly one would expect it to have some z-dependence in the barrier region. What this dependence must be cannot be assumed by such simplified conditions. It is for this reason that this treatment does not assume a form of the eddy viscosity, but rather calculates it from empirical velocities established by Nagabhushaniah. To this end the momentum-conservation equation is employed.

Velocities

Rejection of the error-function solution of Plate has led us to derive our own characterization

of the velocity profiles in the region around the barrier. This characterization is purely empirical, being based on the data of Nagabhushaniah. Several points can be noted about the data. First, it is not complete. Velocity measurements at highest plotted values are not equal to the free-stream values, indicating that the plots do not show the entire region of modification of the flow.* In addition there are few measurements in the regions ahead and downstream of the cavity. This has made characterization in these areas highly approximate. Second, the high degree of turbulence inside the cavity made measurement and hence characterization very difficult. As a result we have not attempted to describe the flow inside the cavity.

The characterization of the velocity used here is a simple modification of the background velocity profile. More specifically, for any value of x the background flow that would have crossed the x=constant plane beneath a height equal to the cavity at that x, must augment the background flow above the cavity height. A function whose shape roughly represents the deviation of the Nagabhushaniah profiles from the background flow was selected to modify the background profile. This function is:

$$\bar{u}_d = A(z - z_r + z_m)e^{-\alpha|z-z_r|} \qquad (75)$$

---

* Additional support for this is apparent from planimeter measurements of the velocity profiles taken at various distances downstream in the same flow. Continuity requires the area under each vertical profile to be equal. The inequality of these areas under the plotted profiles again indicates values different from the free stream in regions not plotted.

The velocity profile then becomes:

$$\bar{u} = \bar{u}_b + \bar{u}_d \tag{76}$$

Here $\bar{u}_b$ is the background power-law profile. Eq. 75 appears to contain four functions of x to be determined empirically; that is, A, z_r, z_m, and α. However, z_r is specified arbitrarily and only A, z_m, and α are determined from the empirical data and continuity relation. This specification facilitates calculation while not disturbing accuracy. The conditions which determine the three functions of x are:

$$\bar{u} = U_q \quad @ \quad z = z_q \tag{77}$$

$$\frac{\partial \bar{u}_d}{\partial z} = 0 \quad @ \quad z = z_p \tag{78}$$

$$\int_{z_c}^{\infty} \bar{u}_d dz = \int_{o}^{z_c} \bar{u}_b dz \tag{79}$$

Here z_q and U_q are the height and value of a measured velocity, z_p is the height at which the profile reaches its maximum positive deviation from the background profile, and z_c is the cavity height; the cavity has been determined by Nagabhushaniah to be roughly ellipsoidal in the region downstream of the barrier, dropping off much more rapidly than the ellipsoidal shape. In addition, to achieve continuous x-derivatives of the velocity, z_c has been smoothed at its reattchment point (twelve times the barrier height). The profiles also contain a discontinuity in the z-derivative at $z=z_r$; this also has been removed by averaging. The profiles calculated by this method are plotted for the typical case given by

the parameters:

$$\bar{u} = 5\ h_b/\text{sec} \quad @ \quad z = 10\ h_b$$

$$p = 1/7$$

in Fig. 10. The technique used in calculating these velocities is outlined in Appendix 3, but we note here that in this, and all other plots included in this section, we have nondimensionalized the length scale with the barrier height, h_b. Comparison of these velocity profiles with the data of Nagabhushaniah indicates good agreement in the region above the cavity. Ahead of the cavity our accuracy may certainly be questioned. Downstream of the cavity, general agreement is obtained, although sufficient data are not available for verification.

Pressure Gradients

Since it is desired to use these velocity values in calculating turbulence characteristics via the momentum-conservation equation, the question of pressure effects is crucial. Although the preceding cases were solved with the assumption of a zero pressure gradient, here pressure effects are obviously present as indicated by the flow separation. The lack of available data regarding the pressure field around the cavity has led us to derive an independent approximation for it based on the potential- (or inviscid-) flow solution for an appropriatly modified geometry. The potential-flow solution is obtained for flow over a solid surface having a shape defined by the zero-velocity function, $z_i(x)$, which is the height inside the cavity at which the velocity drops

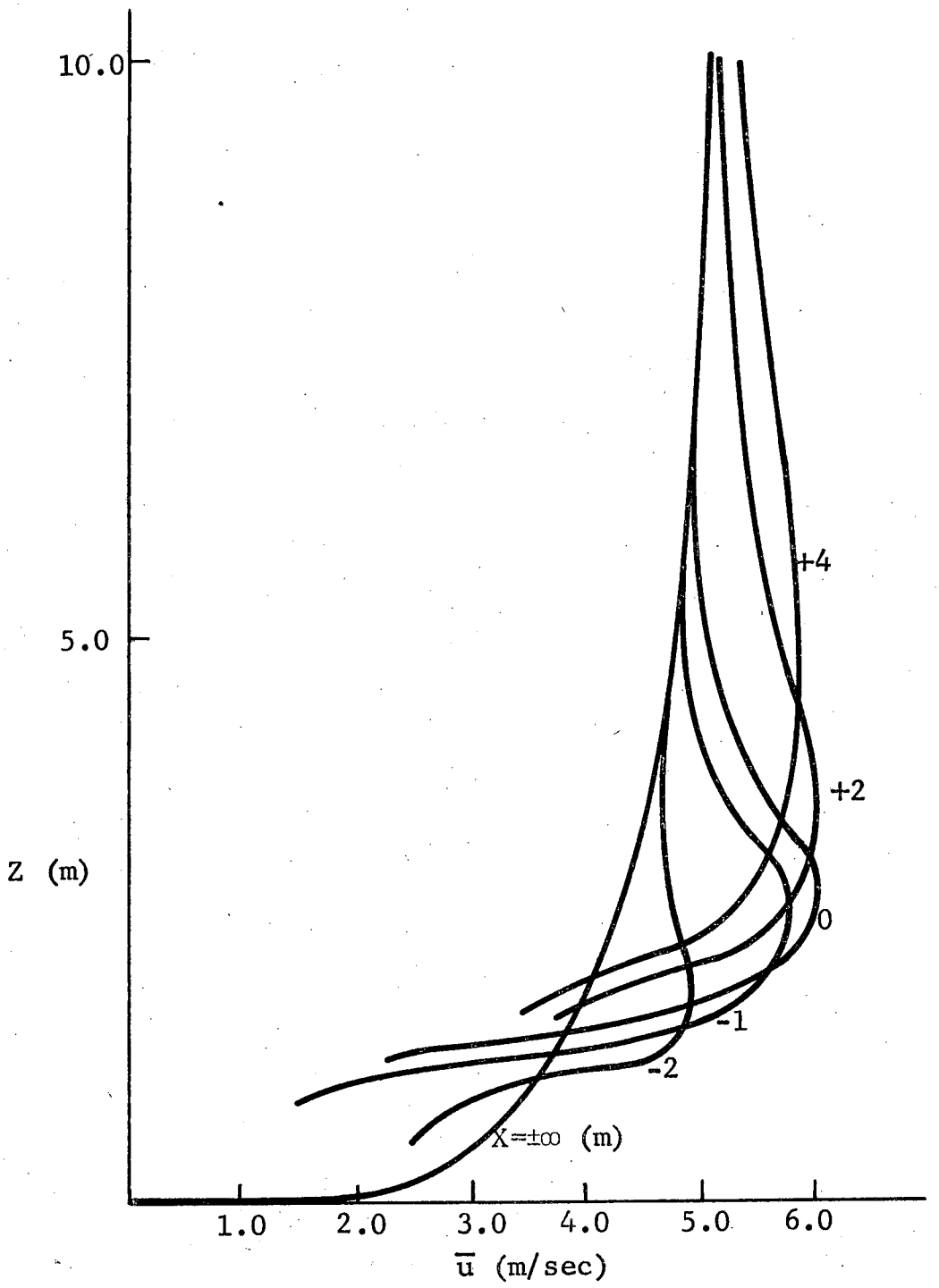

Fig. 10A: Velocity Profiles for Flow Over a Barrier (from x=-∞ to x=+4)

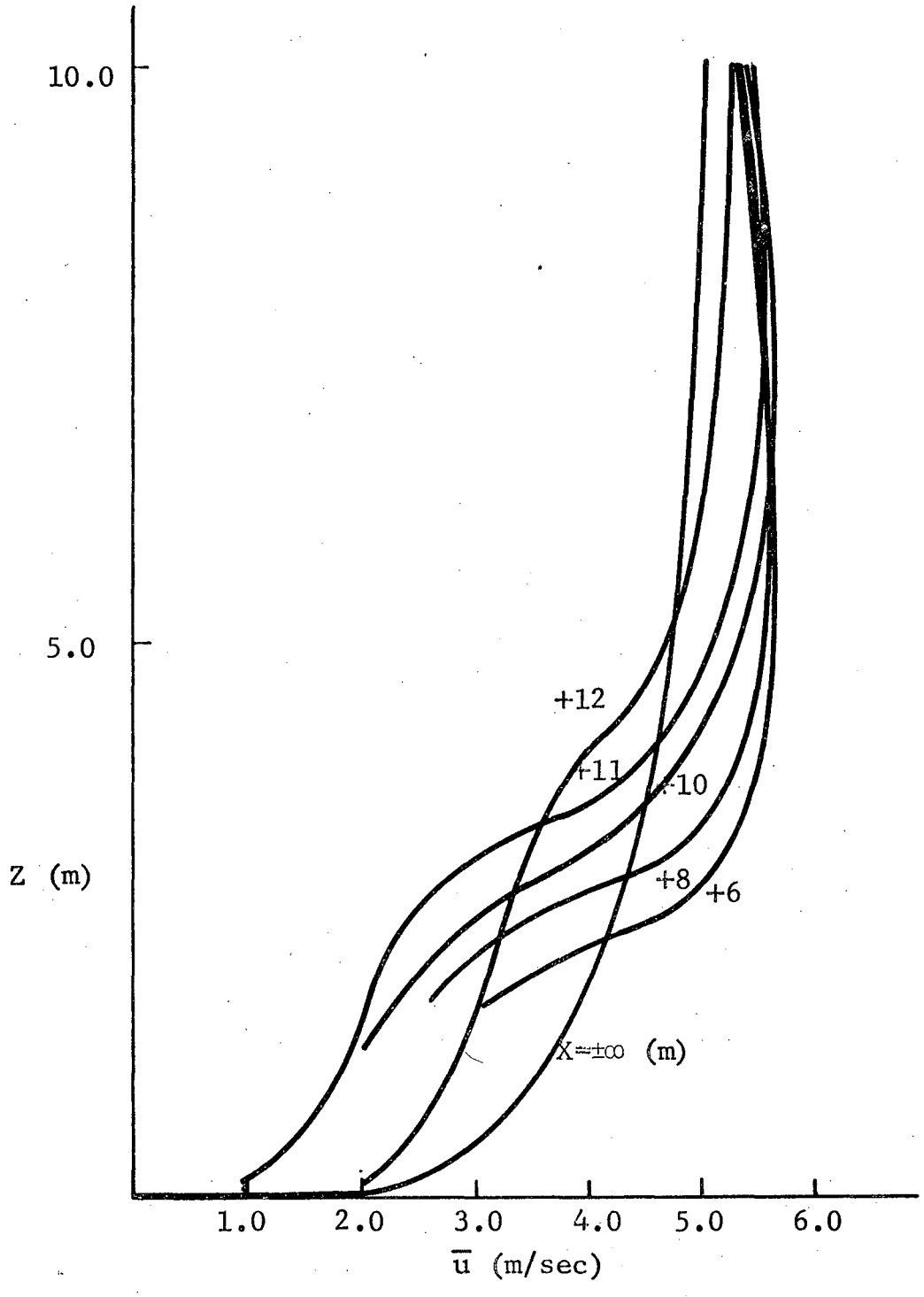

Fig. 10B: Velocity Profiles for Flow Over a Barrier (from x=+6 to x=+∞)

to zero. The rationale of this approach is that the exterior flow "sees" an effective boundary of this shape. The pressure gradients, calculated by a two-dimensional Bernouilli equation,

$$\frac{1}{\rho}\frac{\partial \overline{P}}{\partial x} = U_p\frac{\partial U_p}{\partial x} + W_p\frac{\partial W_p}{\partial x} \qquad (80)$$

are plotted in Fig. 11. Here U_p and W_p are the horizontal and vertical potential flow velocities. A complete discussion of the solution technique used for calculating Fig. 11 is given in Appendix 3. A better source of pressure values in the future will be essential for accurate solutions of the momentum-conservation equation; however, with the stated approximation, we now have sufficient information to achieve a tentative solution in the present system.

Eddy Diffusivities

The relations for momentum conservation in two dimensions, Eqs. 14 and 16, are simplified by neglecting molecular viscosity and body forces, assuming steady state, and ignoring y-derivatives:

$$\overline{u}\frac{\partial \overline{u}}{\partial x} + \overline{w}\frac{\partial \overline{u}}{\partial z} + \frac{\partial \overline{u'^2}}{\partial x} + \frac{\partial \overline{u'w'}}{\partial z} + \frac{1}{\rho}\frac{\partial \overline{P}}{\partial x} = 0 \qquad (81)$$

$$\overline{u}\frac{\partial \overline{w}}{\partial x} + \overline{w}\frac{\partial \overline{w}}{\partial z} + \frac{\partial \overline{u'w'}}{\partial x} + \frac{\partial \overline{w'^2}}{\partial z} + \frac{1}{\rho}\frac{\partial \overline{P}}{\partial z} = 0 \qquad (82)$$

The equations contain three unknowns, hence are not solvable without further assumptions. Because our vertical velocities are not a measured quanity, but are calculated from continuity, we choose to neglect Eq. 82 and use only Eq. 81. Further impetus for this is given by the secondary role of vertical momentum

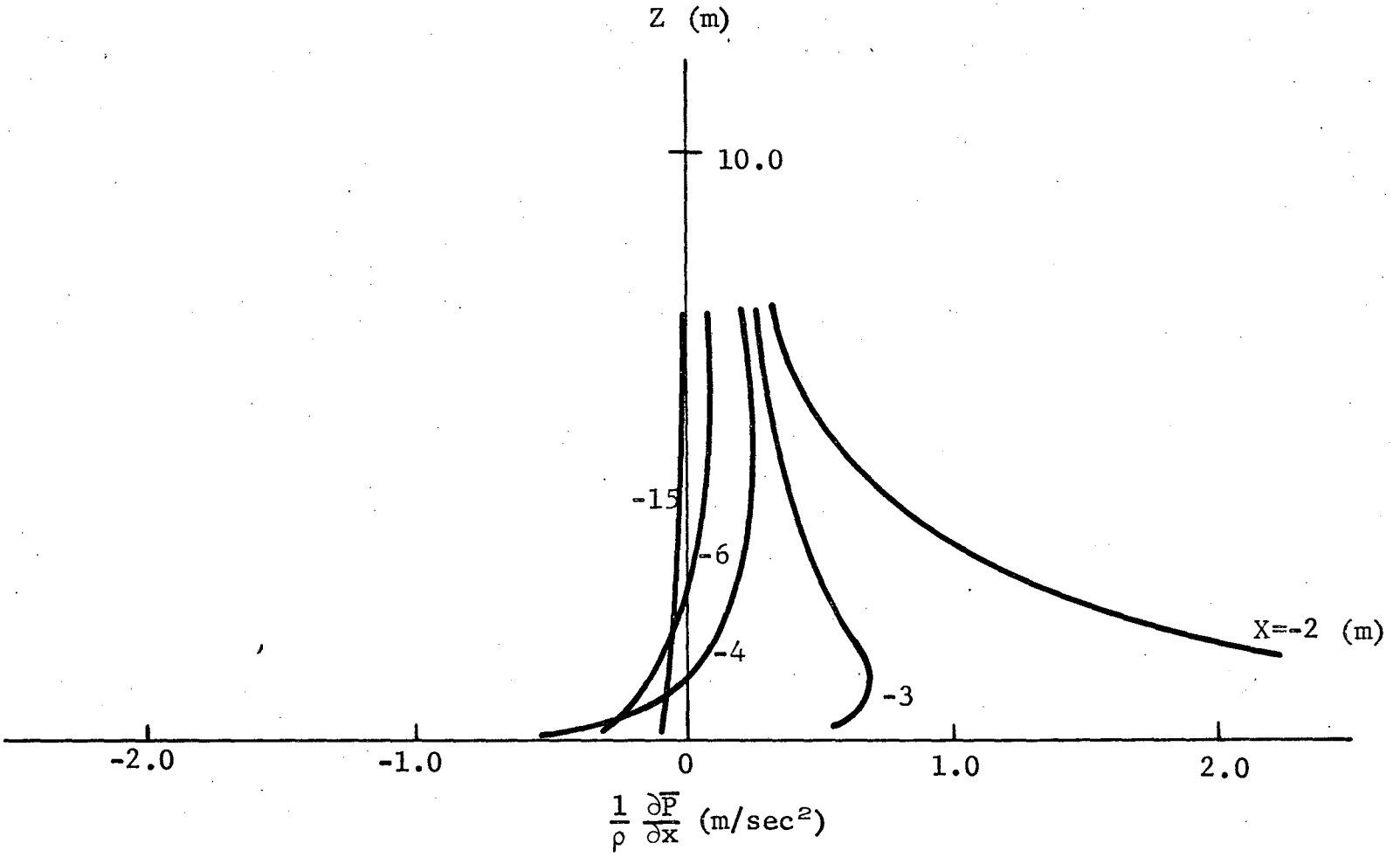

Fig. 11A: Pressure Gradients for Flow Over a Barrier (from x=-15 to x=-2)

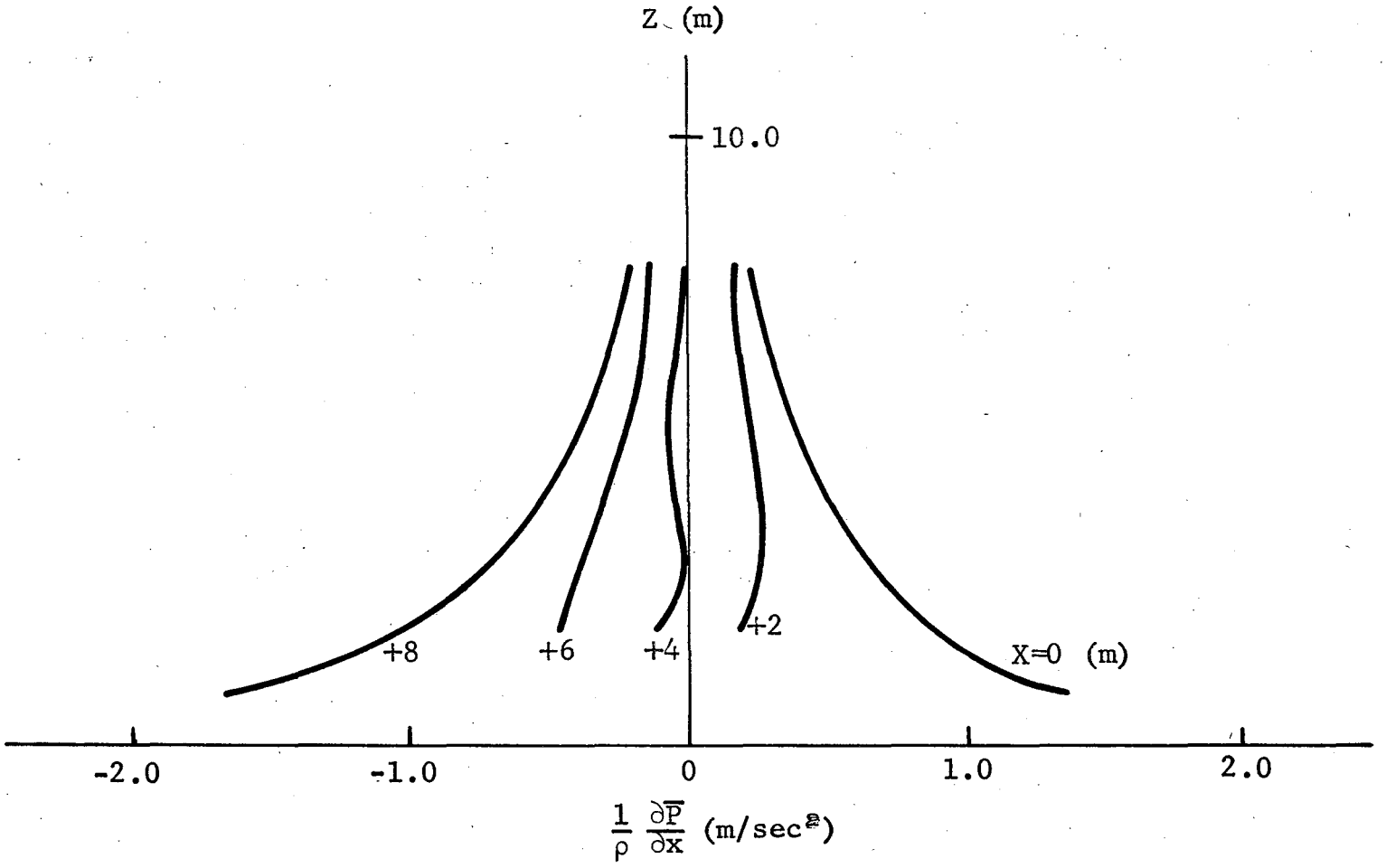

Fig. 11B: Pressure Gradients for Flow Over a Barrier (from x=0 to x=+8)

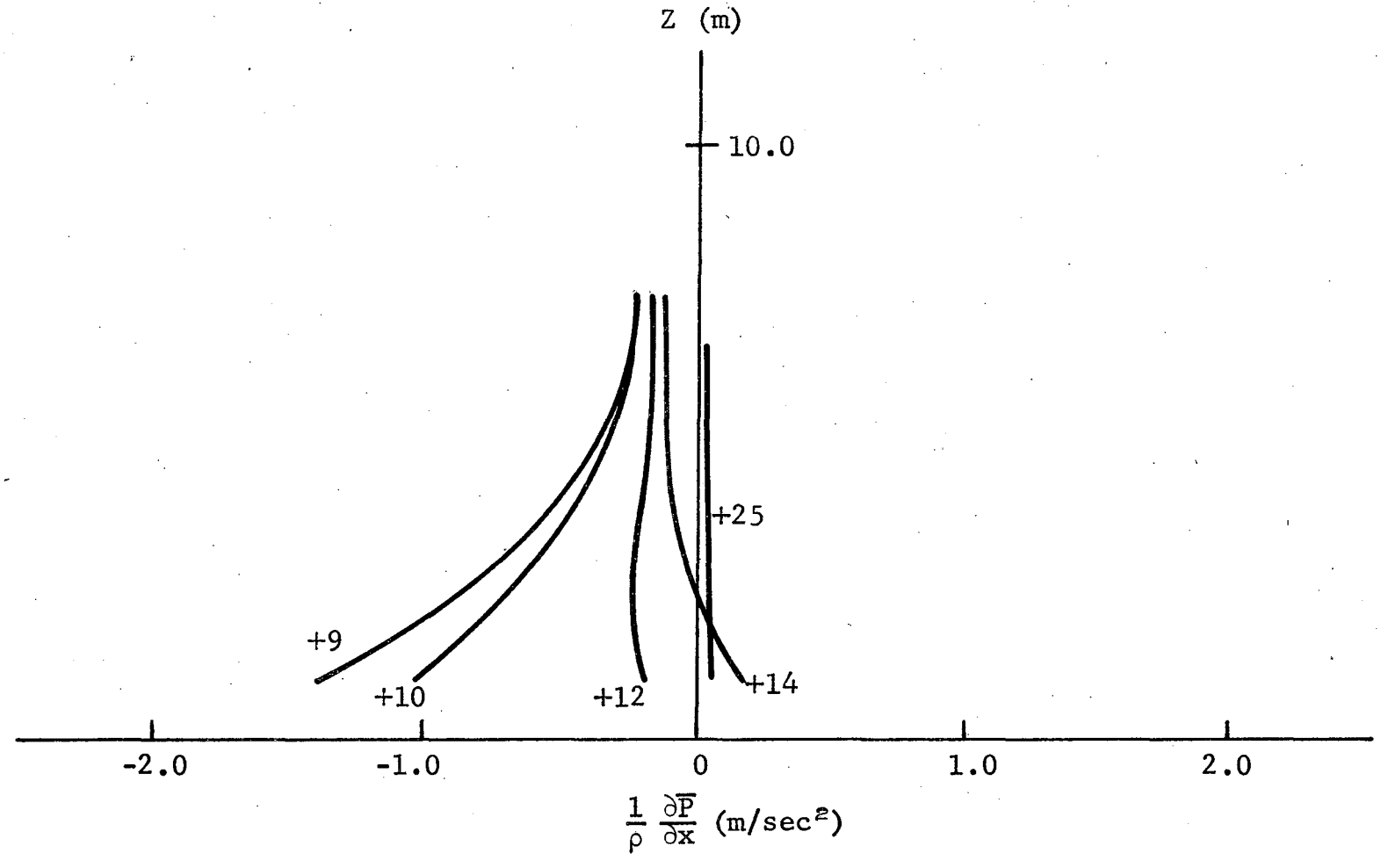

Fig. 11C: Pressure Gradients for Flow Over a Barrier (from x=+9 to x=+25)

in generating turbulence. To complete the solution of Eq. 81, a relation between $\overline{u'^2}$ and $\overline{u'w'}$ is needed. Chang's data[54] on the turbulence characteristics for flow over the cavity shows that these two terms are oppsite in sign and roughly proportional in magnitude.

$$\overline{u'w'} = -f\overline{u'^2} \tag{83}$$

As there is no available way at present to evaluate the functionality of f, it is used here as a constant. Eq. 81 then becomes:

$$\bar{u}\frac{\partial \bar{u}}{\partial x} + \bar{w}\frac{\partial \bar{u}}{\partial z} + \frac{\partial \overline{u'^2}}{\partial x} - f\frac{\partial \overline{u'^2}}{\partial z} + \frac{1}{\rho}\frac{\partial \bar{P}}{\partial x} = 0 \tag{84}$$

Eq. 84 is a linear first-order partial differential equation in two dimensions with constant coefficients, and yields to the method of characteristics for solution. Let

$$\tau = \overline{u'^2} \tag{85}$$

$$T = \bar{u}\frac{\partial \bar{u}}{\partial x} + \bar{w}\frac{\partial \bar{u}}{\partial z} + \frac{1}{\rho}\frac{\partial \bar{P}}{\partial x} \tag{86}$$

then

$$\frac{\partial \tau}{\partial x} = -f\frac{\partial \tau}{\partial z} + T = 0 \tag{87}$$

$$d\tau = \frac{\partial \tau}{\partial x}dx + \frac{\partial \tau}{\partial z}dz \tag{88}$$

$$d\tau = -Tdx + (fdx + dz)\frac{\partial \tau}{\partial z} \tag{89}$$

Hence, along lines defined by $fdx + dz = 0$, and therefore by $z = -fx + c$, we find:

$$\frac{\partial \tau}{\partial x} = -T \tag{90}$$

Fig. 12 shows a plot of T as a function of z and x. The technique for establishing values of $\overline{u'^2}$, or τ, from these values of T is to integrate Eq. 90 along lines defined by $z = -fx + c$. Allthat remains is to establish a value of f and a boundary condition for Eq. 90. Chang's data indicate a value of f between 0.25 and 0.5. We have investigated the solution for both $f = 0.25$ and $f = 0.5$. The data of Chang may also be used to specify a boundary condition for Eq. 90. The most convenient condition is that the values of τ must become negligible at far distances upstream and far above the cavity. This clearly is unrealistic for atmospheric applications, as a non-negligible background value of $\overline{u'^2}$ is usually present in the atmosphere. This raises the question of the relevance of Chang's data to these applications.

The present analysis incorperates the assumption that a proportionality exists between $\overline{u'^2}$ and $\overline{u'w'}$, although the correct value of the proportionality constant, f, remains in qustion. Finally, the question of the boundary condition is resolved by assuming that the values of τ must drop to finite "background" levels established by consideration of the uniform-flat-plate case. Referring to Eq. 20 and neglecting laminar viscosity, we find:

$$\frac{\tau_o}{\rho} = -\overline{u'w'} \tag{91}$$

Again using the definition of u^* as $(\tau_o/\rho)^{\frac{1}{2}}$ we find:

$$-\overline{u'w'} = u^{*2} \tag{92}$$

Thus as a boundary condition for the present case we may use Eq. 83 to assert:

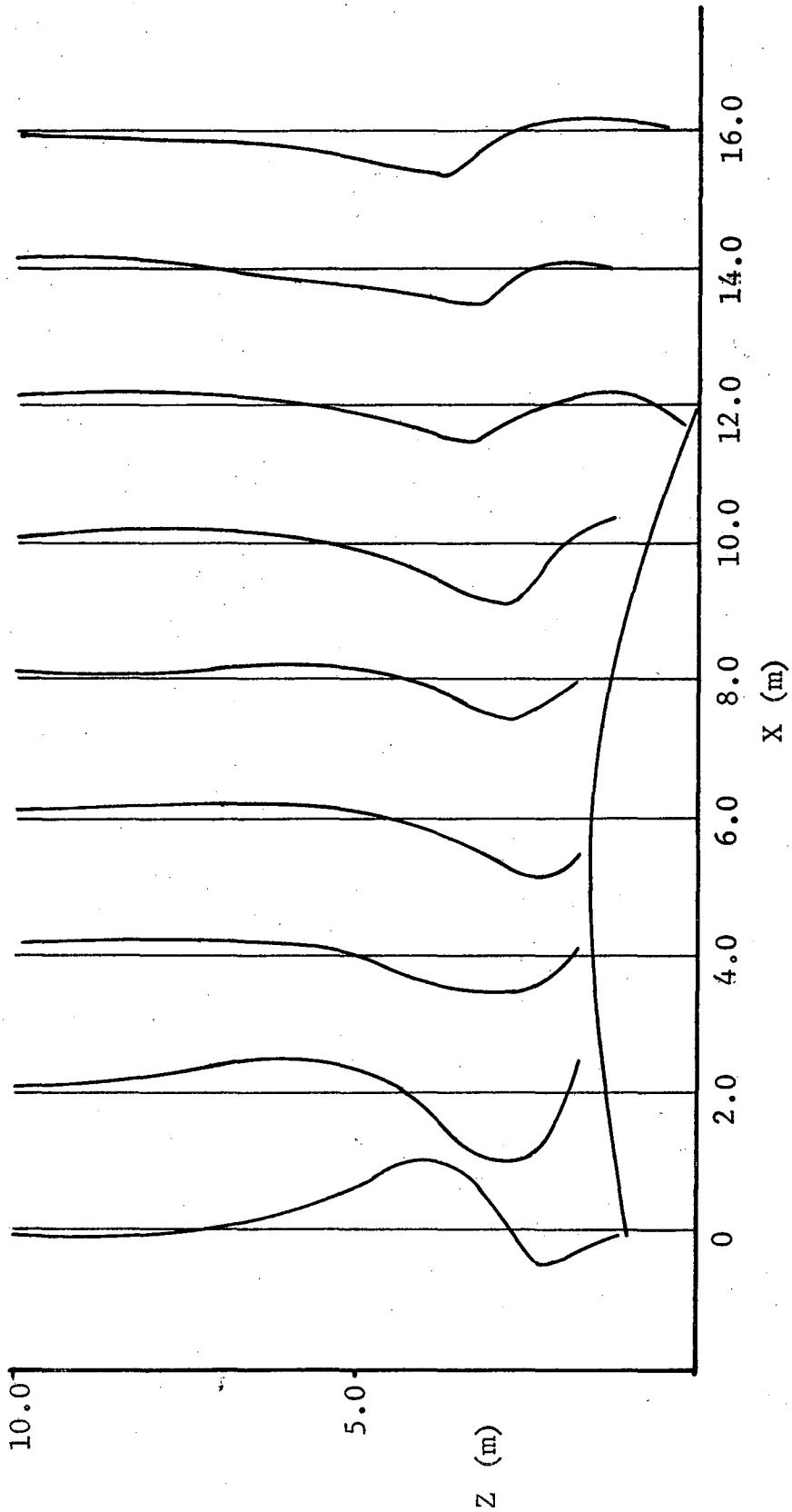

Fig. 12: T (see Eq. 86) as a Function of X and Z

$$\overline{u'^2} = \frac{u^{*2}}{f} \quad \text{as} \quad x \to -\infty \qquad (93)$$

Again remembering that all methods of determining u^* in the atmosphere show its value to lie between 0.1 and 1.0 m/sec[19], we find the background values of $\overline{u'^2}$ to lie between 0.04 and 4.0 m^2/sec^2 for $f = 0.25$ and between 0.02 and 2.0 m^2/sec^2 for $f = 0.5$.

A trial case has been solved for both values of f using a barrier height of 1m. The velocity profiles of Fig. 10 and the pressure-term profiles of Fig. 11 apply in these calculations. In addition, a value of $0.25\ h_b^2/sec^2$ was used as the boundary condition for $\overline{u'^2}$ in solving Eq. 90. Figs. 13 and 14 represent the solution of $\overline{u'^2}$ as a function of x and z, for $f = 0.25$ and $f = 0.5$ respectively. Appendix 3 contains a complete discussion of the solution technique used.

It will be noted immediatly that the values of $\overline{u'^2}$ are higher for the case of $f = 0.25$. This results from the smaller slope of the characteristic lines in that case. To arrive at a given height, the integration must be carried out for a greater horizontal distance in the $f = 0.25$ case.

Both plots show a peak value of $\overline{u'^2}$ in the vertical profiles which rises and spreads out with downstream distance. The only available data for verification are those of Chang, which remain in question. Although numerical agreement is not observed, the presence in Chang's data of a peak which moves upward and spreads out with downstream distance agrees qualitatively with our solutions. As our solutions were aimed at atmospheric situations, atmospheric data must be taken to verify the solution technique.

The solutions themselves suffer from several in-

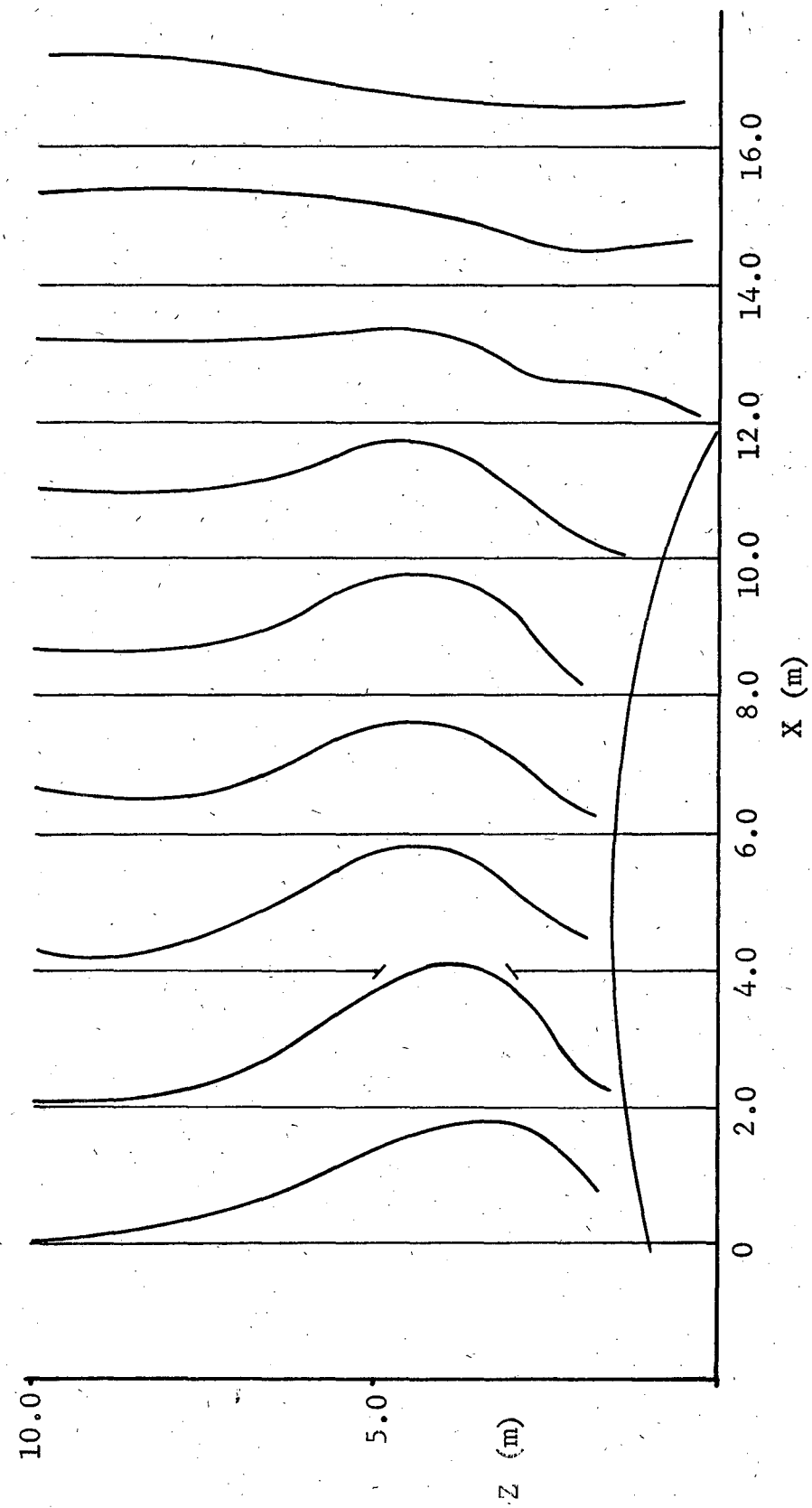

Fig. 13: τ Profiles, Assuming $f = 0.25$

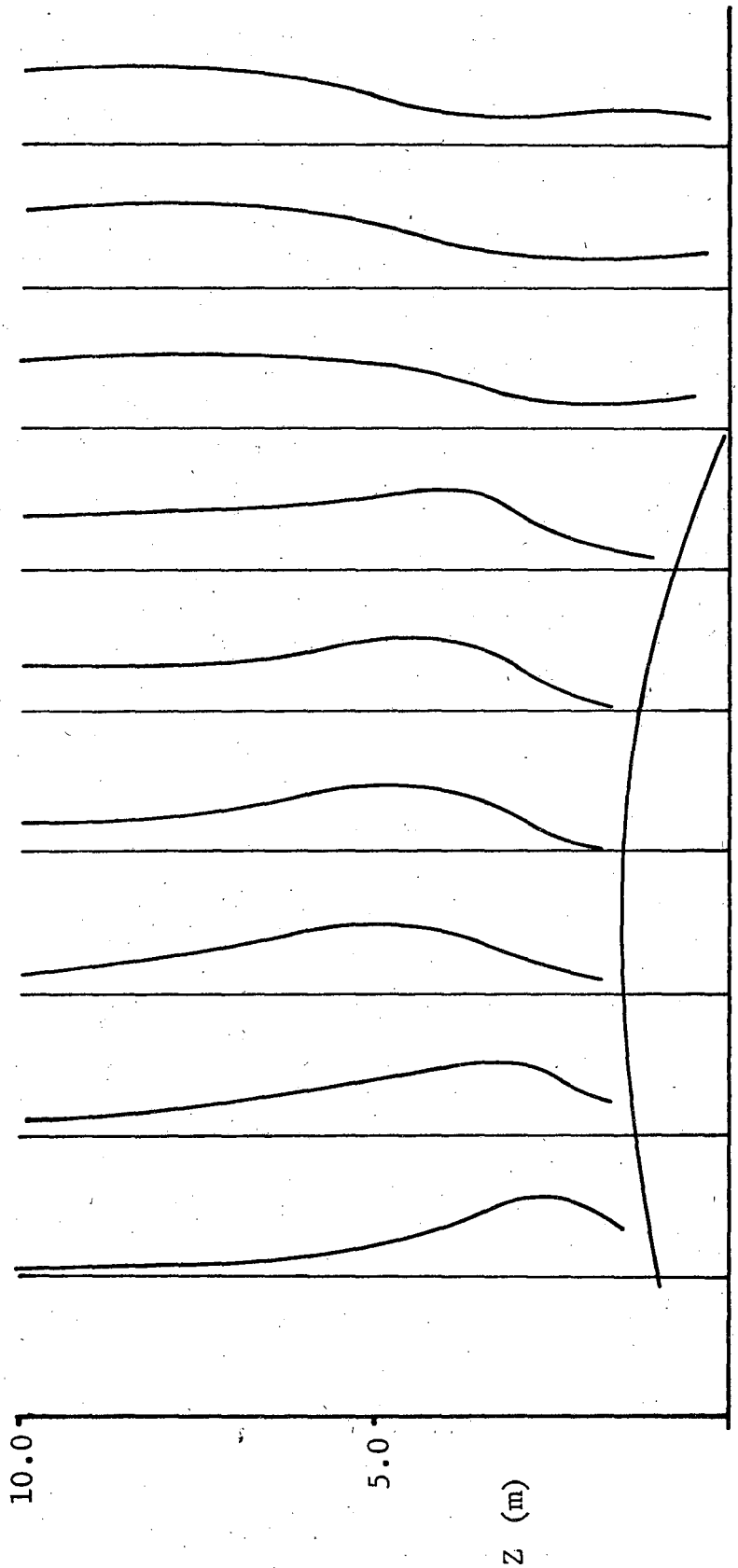

Fig. 14: τ Profiles, Assuming f = 0.5

accuracies. Perhaps the most significant is the inaccuracy in establishing the velocity profiles. Since no atmospheric data were available for these velocities, characterization was based on wind-tunnel studies that were incomplete and inconsistent. Since the solution involves integration of the convection terms of the momentum-conservation equation, small errors may well accumulate. In addition, the pressure term in this equation was approximated from potential flow with no means of verification. This too is integrated along the characteristics, allowing errors to accumulate. Finally, the assumption of proportionality, Eq. 83, is based on data which may have no relation to atmospheric situations. These factors indicate that future treatments should consider establishing turbulence characteristics from methods other than integration of the momentum-conservation equation.

Although we have no means of testing the solutions presented in Figs. 13 and 14, a means for verification might progress through testing their applicability to atmospheric dispersion situations; that is, to establish eddy diffusivities from the solutions, use them in calculating concentration profiles, and perform diffusion experiments to compare with predicted values. To this end, we have calculated concentration predictions from these solutions. Future study will hopefully incorperate the necessary atmospheric diffusion experiments to test these solutions.

We come then to the calculation of eddy diffusivities for which the mass/momentum analogy is used. The eddy diffusivity has units of a velocity times a length. With Prandtl, we postulate that K is the product of a velocity and a mixing length. We further assume that since the mechanism for mass and momentum transfer must be the same, and that since the fluctu-

ating velocities are responsible for the momentum transfer, the velocity contained in the eddy diffusivity is the horizontal component of the turbulent velocity, u', and the length involved is analogous with the logarithmic law:

$$K = kzu' \tag{94}$$

or more practically:

$$K = kz\sqrt{u'^2} \tag{95}$$

The use of u' in this manner implies that areas of high velocity fluctuation correspond to areas of high diffusivity. This is believed to be a realistic picture.

Concentrations

If we neglect the molecular viscosity as well as all y-derivatives and assume steady state, we transform Eq. 12 for the conservation of mass of a particular admixture into

$$\bar{u}\frac{\partial \bar{C}_A}{\partial x} + \bar{w}\frac{\partial \bar{C}_A}{\partial z} + \frac{\partial \overline{u'C_A'}}{\partial x} + \frac{\partial \overline{w'C_A'}}{\partial z} = 0 \tag{96}$$

Making the usual gradient-transport assumption and using an isotropic eddy diffusivity,

$$\overline{u'C_A'} = -K\frac{\partial \bar{C}_A}{\partial x} \tag{97}$$

$$\overline{w'C_A'} = -K\frac{\partial \bar{C}_A}{\partial z} \tag{98}$$

we obtain:

$$\bar{u}\frac{\partial \bar{C}_A}{\partial x} + \bar{w}\frac{\partial \bar{C}_A}{\partial z} = \frac{\partial}{\partial x}\left(K\frac{\partial \bar{C}_A}{\partial x}\right) + \frac{\partial}{\partial z}\left(K\frac{\partial \bar{C}_A}{\partial z}\right) \tag{99}$$

Having the velocities and the eddy diffusivities from the previous considerations, we can solve Eq. 99 for dispersion from a uniformly mixed region of infinite y-extent.

Solution has been carried out using diffusivities calculated for f = 0.25, Fig. 15 and for f = 0.5, Fig. 16. In these calculations the source was located directily above the barrier, and the following input conditions were used:

Source Strength - 1.0
Emission Height - 1.0 h_b
Emission Length - 1.0 h_b

A complete discussion of the solution technique may be found in Appendix 3.

A comparison of Figs. 15 and 16 shows excellent agreement between the two. Although the profiles indicate a slightly greater upward mixing for the f = 0.25 case (Fig. 15), the values are much closer to Fig. 16 than would be expected from a comparison of the turbulence characteristics. This indicates that the concentration profiles are only slightly sensitive to the large changes in diffusivity values generated by the different values of f. One other conclusion concerns the shape of the concentration profiles. Although the velocity and diffusivity profiles differ markedly from background values in the region above the cavity, the resulting concentration profiles maintain a similar shape to those for the uniform-flat-plate flow. The scale is of course different due to the greater height of emission, and much larger diffusivity in the region around the source, but the shape of the profiles indicates similar processes are occurring.

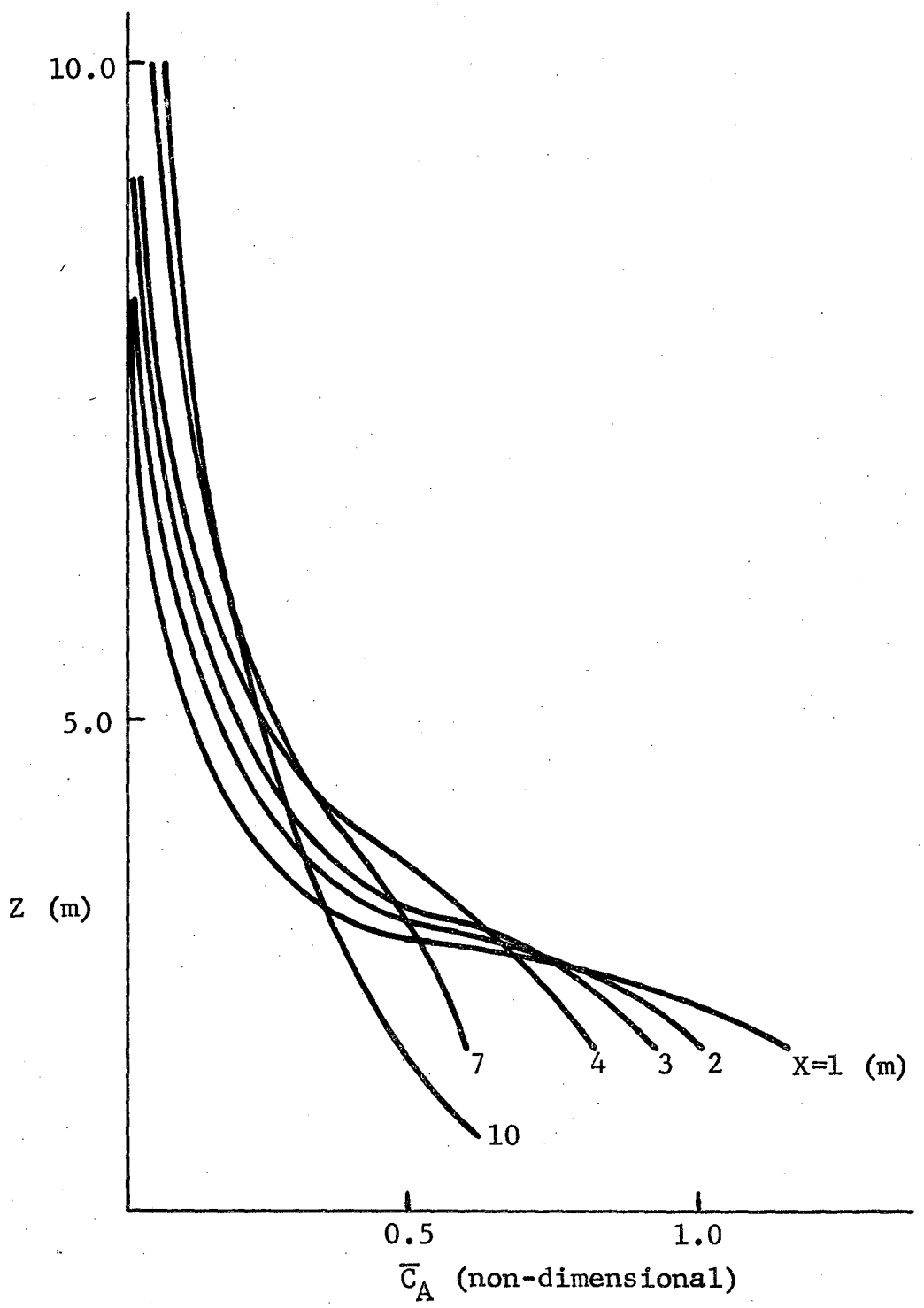

Fig. 15: Concentration Profiles Downstream of a Ground-Level Emission Source for Flow Over a Barrier, Assuming f =0.25

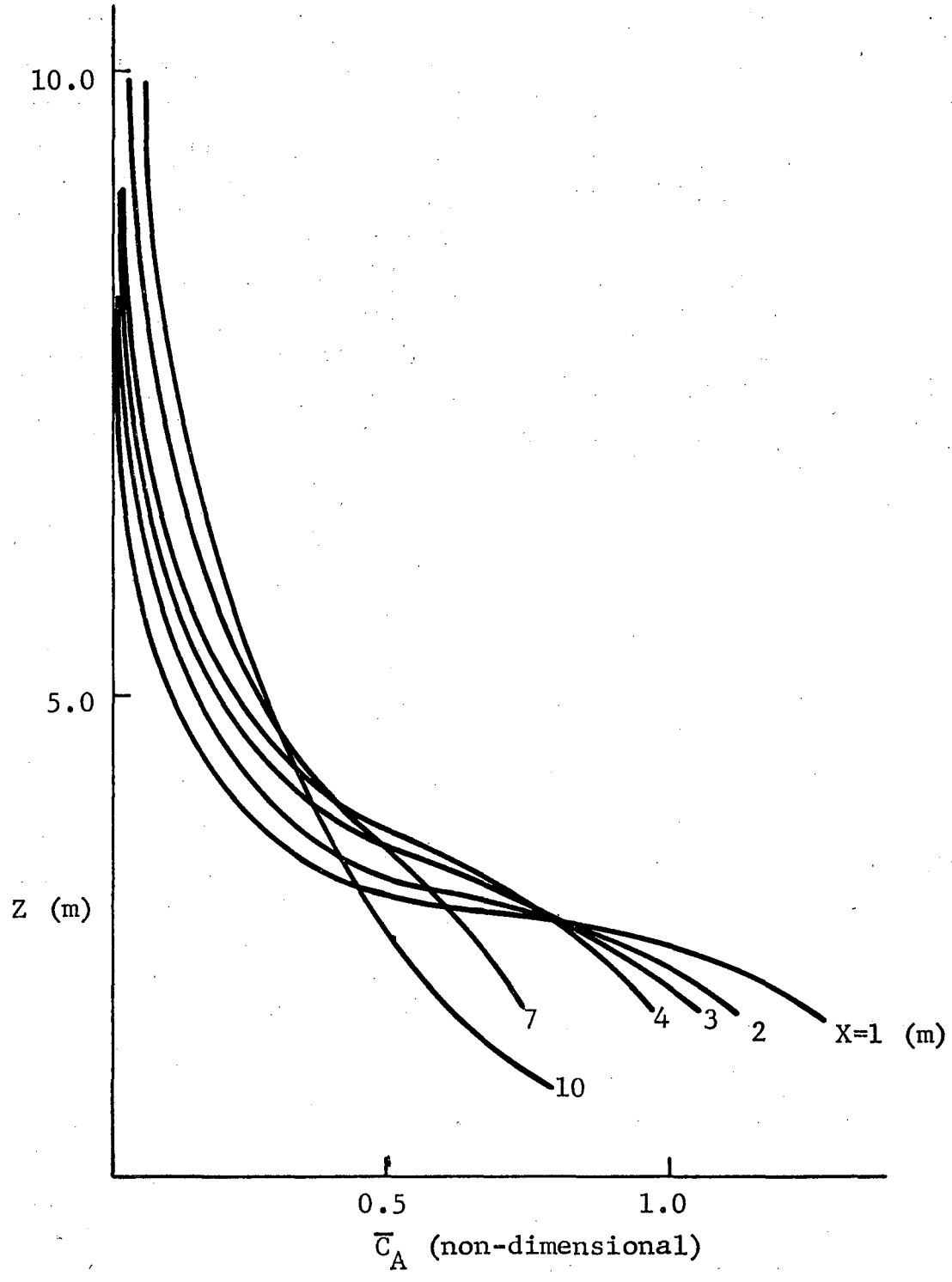

Fig. 16: Concentration Profiles Downstream of a Ground-Level Emission Source for Flow Over a Barrier, Assuming f = 0.5

These observations imply that inaccuracies in the assumptions made to calculate the diffusivities may not be overly detrimental to the results. As no data are available to compare with the predictions of this technique, there is no immediate way of verifying these results. However, the similarity of Figs. 15 and 16 to earlier results encourages further investigation into treating these complicated situations by modification of the simple situations. Future work will hopefully incorperate experimental study that will both verify these results and investigate the possibility of simpler treatment.

IV. CONCLUSION

The work presented here is intended to provide some basis for techniques for handling current freeway-diffusion problems. The use of the conservation-of-momentum equations to solve for the turbulence characteristics of the flow is developed as an alternative to previous characterizations of these terms. For cases where the velocity and pressure terms are well known, this technique provides a means of calculating the fluctuation velocities. These can then be related to the turbulent characteristics of mass transfer, and solution of the diffusion equation in two-dimensional flow is arrived at. Future investigation of the assumptions concerning the turbulence characteristics of these flows will hopefully lead to better answers for these simplified situations.

From the solutions obtained a few important conclusions can be drawn. First, the presented technique calculates concentrations in reasonable agreement with analytic solutions for the uniform-flat-plate case. This does not establish the validity of the technique, but does indicate that it calculates proper values when reduced to the simplified undisturbed boundary-layer case. Second, the analysis of disturbed boundary-layers indicates the possibility that concentration values are not overly sensitive to marked changes in diffusivity. Finally, the concentration calculations for the disturbed boundary-layer cases show that upward motion of contaminants is enhanced by the disruption of the boundary layer, but that the general shape of the profiles is similar to that for the undisturbed case. The implication of the last two conclusions is that more simplified tech-

niques could be used to arrive at similar concentration profiles. Future investigation will hopefully study this possibility.

The relaxation of the general assumptions involving non-neutral atmospheric stability, differential ground heating, highly irregular surface geometries, non-perpendicular wind, etc., is beyond the capabilities of the current technique. It is hoped that the simplified cases that are treated will provide guidelines for solving such more complicated situations, and that such complexities can be handled by minor modifications.

FUTURE CONSIDERATIONS AND SUGGESTIONS

Future study in these areas must involve extensive experimental testing. Primarily we require concentration data, and secondarily, velocity and pressure data. Data are needed for two general purposes: verification, and improvement.

Verification

Data for verification could be concentration measurementsof pollutants emitted in flows discussed previously. If the results are encouraging to the current methods, simpler methods should be investigated, such as considering the barrier as purely a local modification of surface roughness. If the data disagree strongly with calculated predictions, then inprovement of the inputs is necessary.

Improvement

This phase also involves atmospheric testing,

however, here the quanities measured are velocity and pressure. With such additional data, an improvement in the characterization of the velocity and pressure fields can be accomplished. These then can be used to calculate improved values of the diffusivity, and in turn improved prediction of the concentration. Measurements of turbulence characteristics (taken from a statistical analysis of the velocity measurements) will provide a means of checking the assumption of Eq. 83. Establishing the value and functionality of f will enable the technique to improve its calculated value of the diffusivity.

FINAL COMMENTS

If sufficiently accurate values of the input parameters are established, the presented technique should yield correct concentration values. However, the question of how good the input values must be is a crucial consideration; it cannot be answered until proper data are available, but the implications of the answer are clear. If input data must be known to an extreme degree of accuracy to ensure reasonable prediction, the calculational technique developed here would become tremendously cumbersome to apply to real dispersion situations. However, if reasonable prediction can be assured by very rough approximations to the input conditions, then calculational techniques presented here can be used to characterize atmospheric dispersion situations.

REFERENCES

1. Calder, K. L., Eddy Diffusion and Evaporation in Flow Over Aerodynamically Smooth and Rough Surfaces: a Treatment Based on Laboratory Laws of Turbulent Flow with Special Reference to Conditions in the Lower Atmosphere., Quart. J. Mech. Appl. Math., 2, 153-176, 1949.

2. Monin, A. S., and Yaglom, A. M., Statistical Fluid Mechanics, The M.I.T. Press, Cambridge, Mass., p 209, 1971.

3. University of California, Division of Aeronautical Sciences, AS 276 Class Notes, Part I, unpublished, p 16, 1964.

4. Bird, R. B., Stewart, W. E., and Lightfoot, E. N., Transport Phenomena, John Wiley and Sons Inc., New York, 1965.

5. Reference 3, p 33.

6. Plate, E. J., Aerodynamic Characteristics of Atmospheric Boundary Layers, U. S. Atomic Energy Commission Office of Information Services, report No. TID-25465, USAEC Technical Information Center, Oak Ridge, Tenn., p 11, 1971.

7. Reference 6, p 11.

8. Reference 6, p 22.

9. Swinbank, W. C., Structure of Wind and Shearing Stress in the Planetary Boundary Layer, to be published.

10. Klebanoff, P. S., Characteristics of Turbulence in a Boundary Layer with Zero Pressure Gradient, National Advisory Committe for Aeronautics, Annual Report No. 1247, 1955.

11. Reference 2, p 274.

12. Reference 2, p 284.

13. Slotta, L. S., A Critical Investigation of the Universitality of Karman's Constant in Turbulent Flow, H. Lettau, Annual Report, 1963, Department of Meteorology, Univ. of Wisc.

14. Reference 2.

15. Reference 2.

16. Reference 8, p 15.

17. Rosby, C. G., and Montgomery, R. B., The Layers of Frictional Influence in Wind and Ocean Currents, Pap. Phys. Oceanogr. Meteorology, 3(3): 1935.

18. Blackadar, A. K., A Survey of Wind Characteristics Below 1500 ft., Meteorol. Monographs, 4:22, p 3, 1960.

19. Reference 2, p 292.

20. DeMarris, G. A., Wind Speed Profiles at Brookhaven National Laboratory, J. Meteorol., 16:181-190, 1959.

21. Reference 20.

22. Reference 20.

23. Slade, D. H., Meteorology and Atomic Energy 1968, U. S. Atomic Energy Commission, Division of Technical Information, p 80, 1968.

24. Johnson, W. B., Ludwig, F. L., Dabberdt, W. F., and Allen, R. J., Development and Initial Evaluation of an Urban Diffusion Model for Carbon Monoxide, presented at Air Pollution Meteorology Symposium, Sixty-fourth Annual Meeting, Amer. Inst. of Chem. Eng., New York, 1971.

25. Shair, F. H., and Drivas, P. J., Dispersion of a Crosswind Line Source of Tracer Released from an Urban Highway, to be published.

26. Reference 4, p 160.

27. Reference 4, p 160.

28. Sutton, O. G., Micrometeorology, McGraw-Hill Book Co., New York, Toronto, and London.

29. Reference 1.

30. Walters, T. S., The Importance of Diffusion Along the Mean Wind Direction for a Ground-Level Crosswind Line Source., Atmos. Environ., 3: 461-466, 1969.

31. Chatwin, P. C., The Dispersion of a Puff of Passive Contaminent in the Constant Stress Region, Quart. J. of Roy. Meteorol. Soc., 94: 350-360, 1968.

32. Saffman, P. G., The Effect of Wind Shear on Horizontal Spread from an Instantaneous Ground Source, Quart. J. of Roy. Meteorol. Soc., 88:387-393, 1962.

33. Reference 25.

34. Stearns, C. R., and Lettau, H. H., Two Wind-Profile Measurement Experiments in Airflow Over the Ice of Lake Mendota, Annual Report, p115, Univ. of Wisc., Dept. of Meteorol., 1963.

36. Reference 8, p 141-146.

37. Reference 8, p 141-144.

38. Elliot, W. P., The Growth of the Atmospheric Internal Boundary Layer, Trans. Amer. Geophys. Union, 39:1048-1054, 1958.

39. Plate, E. J., and Hidy, G. M., Labotatory Study of Air Flowing Over a Smooth Surface Onto Small Water Waves, J. Geophys. Res., 72:4627-4641, 1967

40. Panofsky, H. A., and Townsend, A. A., Change of Terrain Roughness and the Wind Profile, Quart. J. Roy. Meteorol. Soc., 90: 147-155, 1964.

41. Taylor, P. A., On Wind and Shear-Stress Profiles Above a Chang in Surface Roughness, Quart. J. Roy. Meteorol. Soc., 95:77-91, 1960.

42. Nagabhushaniah, H. S., Separation Downstream of a Plate Set Normal to a Plane Boundary, University Microfilms Inc. Ann Arbor, Mich., 1962.

43. Reference 8, p 160.

44. Schilichting, H., Boundary Layer Theory, Mc Graw-Hill Book Co., Inc., New York, fourth edition, p 689, 1968.

45. Reference 8, p 163.

46. Reference 23, p 225.

47. Reference 23, p 225.

48. Reference 25.

49. Ranzieri, A., California State Division of Highways, Sacramento, private communication.

50. Reference 38.

51. Reference 39.

52. Reference 36.

53. Reference 42.

54. Reference 8, p 163.

TABLE I*

Roughness Parameter, z_o, for Various Surfaces

Surface	z_o (cm)
Scrub Oak, average 30-ft height	100.0
Long grass (60-70 cm) 1.5 m/sec at 2 m	9.0
6.2 m/sec at 2 m	3.7
Mown grass (3 cm)	0.7
Natural snow surface	0.1
Sunbaked sandy alluvium	0.03
Smooth mud flat	0.001
Ocean surface, 10-15 m/sec	0.0021
light wind	0.0010

* From Blackadar, see reference 18.

APPENDIX I

CALCULATIONAL TECHNIQUES USED FOR THE UNIFORM-FLAT-PLATE FLOW

The solution to Eq. 63 using the boundary conditions presented in Eqs. 64-68 was carried out for the typical values of the input parameters outlined in the text. The velocity and diffusivity functions were specified by either the power or logarithmic law, and the corresponding diffusivity function. Eq. 63 was solved using finite difference approximations to the derivatives. These were:

$$\left.\frac{\partial \overline{C}_A}{\partial x}\right|_{i,j} = \frac{\overline{C}_{A_{i,j}} - \overline{C}_{A_{i-1,j}}}{h}$$

$$\left.\frac{\partial \overline{C}_A}{\partial z}\right|_{i,j} = \frac{\overline{C}_{A_{i,j+1}} - \overline{C}_{A_{i,j-1}}}{2k} + \frac{\overline{C}_{A_{i-1,j+1}} - \overline{C}_{A_{i-1,j-1}}}{2k}$$

$$\left.\frac{\partial^2 \overline{C}_A}{\partial x^2}\right|_{i,j} = \frac{\overline{C}_{A_{i,j}} - \overline{C}_{A_{i-2,j}} - \overline{C}_{A_{i-1,j}} + \overline{C}_{A_{i+1,j}}}{2h^2}$$

$$\left.\frac{\partial^2 \overline{C}_A}{\partial z^2}\right|_{i,j} = \frac{\overline{C}_{A_{i,j+1}} + \overline{C}_{A_{i,j-1}} - 2\overline{C}_{A_{i,j}}}{k^2} + \frac{\overline{C}_{A_{i-1,j+1}} + \overline{C}_{A_{i-1,j-1}} - 2\overline{C}_{A_{i-1,j}}}{k^2}$$

Here h and k are the finite difference steps taken in the x- and y-directions respectively. Since Eq. 63 is an elliptic partial differential equation, most numerical solution techniques involve iterative calculations. The solution arrived at here divided the two-dimensional flow field into finite steps, started with zero concentration everywhere except

inside the emission region, and calculated the concentration at each point from Eq. 63 with the finite difference approximations presented. The flow field is proceeded through by calculating a line in the vertical direction, followed by a step in the horizontal direction. The entire flow field flow field is calculated iteratively until convergence is obtained. Eq. 63 with these substitutions becomes:

$$u_j \frac{\overline{C}_{A_{i,j}} - \overline{C}_{A_{i-1,j}}}{h} = K_j \frac{\overline{C}_{A_{i+1,j}} - \overline{C}_{A_{i-1,j}} - \overline{C}_{A_{i,j}} + \overline{C}_{A_{i-2,j}}}{2h^2}$$

$$+ K_j \frac{\overline{C}_{A_{i,j+1}} + \overline{C}_{A_{i,j-1}} - 2\overline{C}_{A_{i,j}} + \overline{C}_{A_{i-1,j+1}} - \overline{C}_{A_{i-1,j-1}} - 2\overline{C}_{A_{i-1,j}}}{2k^2}$$

$$+ \frac{\partial K}{\partial z}\bigg|_j \frac{\overline{C}_{A_{i,j+1}} - \overline{C}_{A_{i,j-1}} + \overline{C}_{A_{i-1,j+1}} - \overline{C}_{A_{i-1,j-1}}}{4k}$$

We rearrange this to form our iteration scheme for calculation of the concentration at a point, i,j, and at iteration r of the flow field.

$$\overline{C}^{(r)}_{A_{i,j}} = \left(\frac{1}{\frac{u}{h} + \frac{K}{2h^2} + \frac{K}{k^2}}\right)\left[\overline{C}^{(r-1)}_{A_{i+1,j}}\left(\frac{K}{2h^2}\right)\right.$$

$$+ \overline{C}^{(r)}_{A_{i-1,j}}\left(\frac{u}{h} - \frac{K}{2h^2} - \frac{K}{k^2}\right) + \overline{C}^{(r)}_{A_{i-2,j}}\left(\frac{K}{2h^2}\right)$$

$$+ \overline{C}^{(r-1)}_{A_{i,j+1}}\left(\frac{K}{2k^2} + \frac{\partial K}{\partial z}\frac{1}{4k}\right) + \overline{C}^{(r)}_{A_{i,j-1}}\left(\frac{K}{2k^2} - \frac{\partial K}{\partial z}\frac{1}{4k}\right)$$

$$\left. + \overline{C}^{(r)}_{A_{i-1,j+1}}\left(\frac{K}{2k^2} + \frac{\partial K}{\partial z}\frac{1}{4k}\right) + \overline{C}^{(r)}_{A_{i-1,j-1}}\left(\frac{K}{2k^2} - \frac{\partial K}{\partial z}\frac{1}{4k}\right)\right]$$

The boundary conditions are implemented by having the finite-difference derivatives go to zero

where specified, and keeping the concentration constant inside the emission region. The calculations were carried out using a CDC 6400 computer. Programs and subroutines were written in FORTRAN IV. The program used for the calculation of the concentration values is given below.

```
      PROGRAM UNIF (INPUT,OUTPUT)
      DIMENSION C(50,50)
      READ 1,N,M,ITR,IMIS,H,HK,U0,ZD,Q,R
    1 FORMAT (4I4,8F5.2)
C THESE ARE THE INPUTS TO THE PROGRAM. N IS THE
C NUMBER OF STEPS IN THE HORIZONTAL DIRECTION, M
C IS THE NUMBER OF STEPS IN THE VERTICAL DIRECTION,
C ITR IS THE NUMBER OF ITERATIONS DESIRED, IMIS IS
C THE X STEP AT WHICH THE EMISSION OCCURS, H AND HK
C ARE THE X AND Y STEP LENGTHS, U0 AND ZD ARE A
C SPECIFIED VELOCITY AND HEIGHT, Q IS THE EMISSION
C STRENGTH, AND R IS THE PROPORTIONALITY COEFFICIENT
C FOR EDDY DIFFUSIVITY.
      NM=N-1
      MM=M-1
      DO 13 I=1,N
      DO 13 J=1,M
      C(I,J)=0.
   13 CONTINUE
      CL=U0/ALOG(ZD/.01)
C THIS CALCULATION IS FOR THE LOG. LAW.
      C(IMIS,1)=Q
      DO 100 II=1,ITR
      PRINT 101,II
  101 FORMAT (/1X,* ITR= *,1I4)
      I=3
      DO 4 J=2,MM
      CALL CAL (C,I,J,H,HK,R,CL)
      C(1,J)=C(3,J)
      C(2,J)=C(3,J)
    4 CONTINUE
      C(3,1)=C(3,2)
      C(2,1)=C(3,2)
      C(3,M)=C(3,MM)
      C(2,M)=C(3,MM)
      DO 5 I=4,NM
      DO 6 J=2,MM
      CALL CAL(C,I,J,H,HK,R,CL)
    6 CONTINUE
      IF (I-IMIS) 7,8,7
    7 C(I,1)=C(I,2)
    8 C(I,M)=C(I,MM)
```

```
    5 CONTINUE
      DO 9 J=1,M
      C(N,J)=C(NM,J)
    9 CONTINUE
C THIS COMPLETES THE BASIC ITERATION IN WHICH THE
C CONCENTRATION IS CALCULATED AT EACH POINT BY CALLING
C THE SUBROUTINE CAL.
      DO 11 I=1,N
      PRINT 10,(C(I,J),J=1,M)
   10 FORMAT (1X,12F10.6)
   11 CONTINUE
  100 CONTINUE
      STOP
      END


      SUBROUTINE CAL (C,I,J,H,HK,R,CL)
      DIMENSION C(50,50)
      Z=J*HK+.01
      ZM=Z-HK/2
      ZP=Z+HK/2
      U=CL*ALOG(Z/.01)
      TD=R*Z/2/H+R*ZM/2/HK+R*ZP/2/HK+U
      C(I,J)=1/TD*(C(I-1,J)*U+R*Z/2/H*C(I-2,J)-R*ZM*(C
     1 (I-1,J)-C(L-1,J-1)-C(I,J-1))/2/HK+R*ZP*(C(I-1,J
     2 +1)-C(I-1,J)+C(I,J+1))/2/HK+R*Z*(C(I+1,J)-C(I-1
     3 ,J))/2/H)
      RETURN
      END
```

APPENDIX II

CALCULATIONAL TECHNIQUES USED FOR FLOW OVER A DISCONTINUITY IN SURFACE ROUGHNESS

The techniques used here are essentially the same as those for the uniform-flat-plate case except for the following added variations in the system:

1. U is now a function of x and must be calculated from the equation system, Eqs. 55a-h.
2. As a result of (1), vertical velocities are now involved and must be accounted for.
3. The eddy diffusivity is also a function of x as well as z.

Calculation of Velocity Profiles

Eqs. 55a-h are solved in the manner outlined in the text for which a subroutine has been developed. This subroutine incorperates a Newton-Raphson algorithm for the simultaneous solution of Eqs. 55a, 55e, 55f, and 55g.

```
      SUBROUTINE VEL (U,W,N,M,Z01,Z02,H,HK,IS,U0,ZD)
      DIMENSION U(50,50),W(50,50),US(50),US2(50),WS(50)
C HERE U AND W ARE THE VELOCITY AND DIFF. FIELDS GIVEN
C TO THE MAIN PROGRAM, N AND M ARE THE NUMBER OF STEPS
C IN THE HORIZONTAL AND VERTICAL DIRECTIONS, Z01,
C AND Z02 ARE THE UPSTREAM AND DOWNSTREAM SURFACE
C ROUGHNESS PARAMETERS, H AND HK ARE THE HORIZONTAL
C AND VERTICAL STEP LENGTHS, IS IS THE HORIZONTAL
C STEP AT WHICH THE DISCONTINUITY OCCURS, AND U0 AND
C ZD ARE THE VELOCITY AND HEIGHT SPECIFIED FOR THE
C UPSTREAM VELOCITY PROFILE.
      REAL N0,N1,N2,N3,N4
      B=ALOG(Z02/Z01)
      N4=B
      N3=2*B**2-4*B
```

```
      N2=B**3-6*B**2+2*B
      N1=-2*B**3
      N0=2*B**2
      P3=2*B
      P2=3*B**2-2*B
      P1=B**3-B**2
      P0=-B**2
C THIS IS JUST NOTATION TO SIMPLIFY THE WRITING OF
C THE POLYNOMIAL APPROXIMATIONS.
      ISM=IS-1
      ISP=IS+1
      CL=U0/ALOG(ZD/Z01)
      DO 2 J=1,M
      Z=J*HK
      US(J)=CL*ALOG(Z/Z01)
      WS(J)=CL*.16*Z
    2 CONTINUE
C THIS IS THE SET UP OF THE UPSTREAM VELOCITY PROFILE.
C HERE US AND WS ARE THE UPSTREAM VELOCITY AND DIFF-
C USIVITY PROFILES.
      DO 3 I=1,ISM
      DO 4 J=1,M
      U(I,J)=US(J)
      W(I,J)=WS(J)
    4 CONTINUE
    3 CONTINUE
      DO 5 I=ISP,N
      X=(I-IS)*H
      F=.16*X
      C=3.
   22 T1=N4*C**4+N3*C**3+N2*C**2+N1*C+N0
      T=Z02*EXP(C)*T1+0.-F*(P3*C**3+P2*C**2+P1*C+P0)
      IF (T) 20,21,21
   21 C=C+1.
      GO TO 22
C WE WISH TO FIND THE ROOT TO T, HENCE FIRST WE STEP
C OFF VALUES OF C AT INTERVALS OF 1. TO FIND AN APPROX-
C IMATE ROOT.  WE WILL NEXT STEP WITH .1, AND THEN
C USE THE NEWTON-RAPHSON TO GET A GOOD VALUE OF C.
   20 C=C+.1
      T1=N4*C**4+N3*C**3+N2*C**2+N1*C+N0
      T=Z02*EXP(C)*T1+0.-F*(P3*C**3+P2*C**2+P1*C+P0)
      IF (T) 20,6,6
    6 CH=C
      T1=N4*C**4+N3*C**3+N2*C**2+N1*C+N0
      T=Z02*EXP(C)*T1+0.-F*(P3*C**3+P2*C**2+P1*C+P0)
      DT=Z02*EXP(C)*(T1+4*N4*C**3+3*N3*C**2+2*N2*C+N1)
     1 -F*(3*P3*C**2+2*P2*C+P1)
      C=C-T/DT
      IF (ABS(C-CH)-.001) 6,6,7
C THIS IS THE MAJOR ROOT FINDING PORTION OF THE PROGRAM.
```

```
C ONCE AN ACCEPTABLE VALUE OF C IS FOUND, WE CAN NOW
C PROCEED TO CALCULATE DELTA, THE INTERNAL BOUNDARY
C LAYER THICKNESS, AND HENCE THE VELOCITY PROFILES
C DOWNSTREAM OF THE DISCONTINUITY.
    7 DEL=Z02*EXP(C)
      JT=DEL/HK
      P=P3*C**3+P2*C**2+C*P1+P0
      D=C**4+C**3*(B-1.)+C**2
      US2(I)=CL*.4*SQRT(ABS(P/D+1.))
      IF (JT) 8,8,9
    8 J1=1
      GO TO 10
    9 J1=JT+1
      DO 11 J=1,JT
      Z=J*HK
      U(I,J)=US2(I)/.4*ALOG(Z/Z02)
      W(I,J)=US2(I)*.4*Z
   11 CONTINUE
   10 DO 12 J=J1,M
      U(I,J)=US(J)
      W(I,J)=WS(J)
   12 CONTINUE
    5 CONTINUE
C FINALLY WE MUST SPECIFY A VALUE OF U AND W FOR THE
C UNDEFINED REGION AROUND THE DISCONTINUITY.  THIS
C IS DONE BY AVERAGING.
      DO 13 J=1,M
      U(IS,J)=(U(ISP,J)+U(ISM,J))/2
      W(IS,J)=(W(ISP,J)+W(ISM,J))/2
   13 CONTINUE
      RETURN
      END
```

Calculation of Concentration Values

The caluclation for concentration values proceeds much the same in the discontinuity case as it did in the uniform-flat-plate case. Again finite difference approximations are used for the derivatives, and again, solution is by iterative calculations over the entire flow field. Here, however, the velocities and diffusivities appear with two subscripts and are calculated separately as outlined previously. Vertical velocities are calculated from the continuity equation. The new iteration scheme is:

$$\bar{C}_{A_{i,j}}^{(r)} = \frac{1}{\frac{u_{i,j}}{h} + \frac{K_{i-1,j}}{2h^2} + \frac{K_{i,j}}{k^2} + \frac{K_{i-1,j}}{k^2}} \Bigg[\bar{C}_{A_{i+1,j}}^{(r-1)} \left(\frac{K_{i,j}}{2h^2}\right)$$

$$+ \bar{C}_{A_{i-1,j}}^{(r)} \left(\frac{u_{i,j}}{h} - \frac{K_{i,j}}{2h^2} - \frac{K_{i-1,j}}{k^2}\right) + \bar{C}_{A_{i-2,j}}^{(r)} \left(\frac{K_{i-1,j}}{2h^2}\right)$$

$$+ \bar{C}_{A_{i,j+1}}^{(r-1)} \left(\frac{K_{i,j}}{2k^2} - \frac{w_{i,j}}{4k} + \left.\frac{\partial K}{\partial z}\right|_{i,j} \frac{1}{4k}\right)$$

$$+ \bar{C}_{A_{i,j-1}}^{(r)} \left(\frac{K_{i,j}}{2k^2} + \frac{w_{i,j}}{4k} - \left.\frac{\partial K}{\partial z}\right|_{i,j} \frac{1}{4k}\right)$$

$$+ \bar{C}_{A_{i-1,j+1}}^{(r)} \left(\frac{K_{i-1,j}}{2k^2} - \frac{w_{i,j}}{4k} + \left.\frac{\partial K}{\partial z}\right|_{i-1,j} \frac{1}{4k}\right)$$

$$+ \bar{C}_{A_{i-1,j-1}}^{(r)} \left(\frac{K_{i-1,j}}{2k^2} + \frac{w_{i,j}}{4k} - \left.\frac{\partial K}{\partial z}\right|_{i-1,j} \frac{1}{4k}\right) \Bigg]$$

(Here $w_{i,j}$ is actually an average of $w_{i,j}$ and $w_{i-1,j}$ which has been simplified for ease in notation)

The implemetation of this iteration scheme in the computer program to calculate the concentrations differs very little from the program for the uniform-flat-plate case, hence we will not present the entire program here. The major differences are that the velocities are calculated from the subroutine, VEL, presented previously, and a new subroutine to calculate the actual concentrations at specific points, CAL, was developed.

```
      SUBROUTINE CAL (C,I,J,H,HK,U,D,V)
      DIMENSION C(50,50),U(50,50),D(50,50)
C HERE U IS THE VELOCITY GRID, D IS THE DIFFUSIVITY
C GRID, BOTH CALCULATED FROM SUBROUTINE VEL, AND
C V IS THE VERTICAL VELOCITY AT I,J.  THE MAIN PROGRAM
C SETS V EQUAL TO ZERO AT THE TOP OF THE FLOW FIELD,
C AND ELSEWHERE IT IS CALCULATED BY THIS SUBROUTINE,
C AND CARRIED BACK AND FORTH FROM THE MAIN PROGRAM
C AS EACH VERTICAL STEP IS PROGRESSED.
      VP=V-(U(I,J)-U(I-1,J))*HK/H
      VM=V
      V=VP
```

```
C THIS IS THE CALCULATION OF THE VERTICAL VELOCITY
C FROM THE CONTINUITY RELATION.  A NEW VALUE OF V
C IS CALCULATED AND PLACED IN VP WHILE THE OLD VALUE
C IS CARRIED OVER INTO VM.
      DM=(D(I,J)+D(I-1,J)+D(I-1,J-1)+D(I,J-1))/4
      DP=(D(I,J)+D(I-1,J)+D(I-1,J+1)+D(I,J+1))/4
      TD=D(I-1,J)/2/H-VM/4+DM/2/HK+DP/2/HK+VP/4+U(I,J)
      C(I,J)=1/TD*(U(I-1,J)*C(I-1,J)+D(I-1,J)*C(I-2,J)
     1 /2/H+VM/4*(C(I,J-1)+C(I-1,J)+C(I-1,J-1))-DM/2/H
     2 K*(C(I-1,J)-C(I,J-1)-C(I-1,J-1))+DP/2/HK*(C(I,J
     3 +1)+C(I-1,J+1)-C(I-1,J))-VP/4*(C(I,J+1)+C(I-1,J
     4 +1)+C(I-1,J))+D(I,J)/2/H*(C(I+1,J)-C(I-1,J)))
      RETURN
      END
```

APPENDIX III

CALCULATIONAL TECHNIQUES USED FOR FLOW OVER A BARRIER

The treatment of flow over a barrier differs considerably from the other cases in the velocity and pressure calculations; however, the concentration calculations remain basicly the same.

Calculation of Velocity Profiles

The velocity is characterized by the Eqs. 75 and 76; the constants being determined by Eqs. 77-79. The calculation of the constants from Eqs. 77-79 was accomplished by a Newton-Raphson algorithm. The flow field was divided into finite steps and the necessary constants were calculated for each x-step. The profile was then calculated at each y-grid point. A computer subprogram was developed to accomplish this solution, and is presented below. The program calculates horizontal velocities and stores them in the array, U(I,J), and establishes vertical velocities from the continuity relation and stores them in the array, W(I,J). In order to calculate accurate vertical velocities, it was necessary to carry out the calculation of horizontal velocities to four times the height of the flow field. This was necessary because the implemetation of the continuity equation uses the boundary condition that the vertical velocity is zero at some height sufficiently far above the surface. This was found to be four times the height we were interested in considering.

```
      SUBROUTINE PROFIL (N,M,MW,IF,H,HK,C1,C2,U,W,ZE)
      DIMENSION U(50,50),W(50,50),UP(80),UM(80),WT(80)
     1 ,U0(80),ZE(50)
```

```
C N AND M ARE THE HORIZONTAL AND VERTICAL DIMENSIONS
C OF THE FLOW FIELD, MW IS THE NUMBER OF STEPS TAKEN
C IN THE VERTICAL DIRECTION TO INSURE VALIDITY OF
C CONTINUTIY TREATMENT, IF IS THE X STEP AT WHICH
C THE BARRIER IS PLACED, H AND HK ARE THE HORIZONTAL
C AND VERTICAL STEP LENGTHS, C1 AND C2 ARE CONSTANTS
C USED IN DETERMINING THE SHAPE OF THE CAVITY, ZE IS
C THE CALCULATED CAVITY SHAPE AS A GUNCTION OF X, AND
C UP, UM, AND U0 ARE ALL TEMPORARY STORAGE REGISTERS
C FOR THE VERTICAL AND HORIZONTAL VELOCITY DETERMINATION.
      NM=N-1
      MM=M-1
      P=1./7
C WE USE A VALUE OF 1/7 FOR P IN THE BACKGROUND PROFILE.
      CL=5./10.**P
      ZC=0.
      DO 9 I=1,N
      ZH=ZC
      X=(I-IF)*H
      IF (X) 40,41,41
   40 ZC=1.04252726/EXP(.440239478*(X-.3075754621)**2)
      GO TO 13
   41 IF (X-12.) 30,12,12
   30 zc=C1*SQRT(1.-(X-4.7)**2/C2**2)+1.6-C1
      IF (ZC) 12,13,13
   12 ZC=0.
C THIS IS THE CALCULATION OF THE CAVITY SHAPE.  ZC WILL
C NOW BE PUT INTO ZE(I).
   13 C=CL*ZC**(P+1.)
      ZE(I)=ZC
      IF (X+2.) 42,42,43
   42 ZP=1.5
      ZX=1.0
      ZV=.659
      GO TO 44
   43 ZP=.4775*(X+2.)**.85+1.5
      ZX=.125*(X+2.)+1.
      ZV=.659*(X+3.)**.283
   44 IF (X) 16,17,17
   16 FV=-3./EXP(.35*X**2)-2./EXP(.015*(X-12.)**2)
      GO TO 20
   17 FV=-3./EXP(.122*X**2)-2./EXP(.015*(X-12.)**2)
C THIS IS THE SPECIFICATION OF THE CONDITIONS NECESSARY
C TO ESTABLISH THE CONSTANTS.
   20 FH=0.
      A=.1
    3 F=A*(ZP-ZC)/EXP(A*ABS(ZC-ZX))+2.+2*(ZX-ZP)*A-C*A
     1 /FV*(ZV*A-ZP*A+1.)/EXP(A*ABS(ZV-ZX))
      IF (ABS(F+FH)-ABS(F-FH)) 2,1,1
    1 A=A+.1
      FH=F
      GO TO 3
C THIS IS A STEP-OFF TO DETERMINE AN APPROXIMATE
```

```
C ROOT.  A MORE EXACT ROOT WILL BE DETERMINED NEXT
C BY THE NEWTON-RAPHSON ALGORITHM.
    2 A=A-.1
    5 AH=A
      F=A*(XP-ZC)/EXP(A*ABS(ZC-ZX))+2.+2*(ZX-ZP)*A-C*A
     1 /FV*(ZV*A-ZP*A+1.)/EXP(A*ABS(ZV-ZX))
      DF=(ZP-ZC)/EXP(A*ABS(ZC-ZX))*(1.-A*ABS(ZX-ZC))+2
     1 *(ZX-ZP)-C/FV/EXP(A*ABS(ZV-ZX))*(2*ZV*A-2*ZP*A+
     2 1.-A*(ZV*A-ZP*A+1.)*ABS(ZV-ZX))
      A=A-F/DF
      IF (ABS(A-AH)-.0001) 4,4,5
    4 PRINT 6,A
    6 FORMAT (1X,* A= *,1F10.4)
      ZM=1./A+ZX-ZP
      AC=FV/(ZV-ZX+ZM)*EXP(A*ABS(ZV-ZX))
C NOW THAT WE HAVE ALL THE NECESSARY CONSTANTS, WE
C WILL CALCULATE THE VERTICAL VELOCITY PROFILE.
      DO 18 J=2,MW
      IF(I-1) 19,19,31
   31 IF (I-2) 32,32,33
   33 UM(J)=U0(J)
   32 U0(J)=UP(J)
   19 Z=(J-1)*HK
      UP(J)=CL*Z**P+AC*(Z-ZX+ZM)/EXP(A*ABS(Z-ZX))
   18 CONTINUE
      IF (I-1) 9,9,34
   34 IF (I-2) 9,9,35
   35 WT(MW)=0.
      DO 36 J=3,MW
      L=MW-J+2
      WT(L)=WT(L+1)+(UP(L)-UM(L)+UP(L+1)-UM(L+1))*HK/4
     1 /H
   36 CONTINUE
      DO 37 J=1,MM
      U(I-1,J)=U0(J)
      W(I-1,J)=WT(J)
   37 CONTINUE
      U(I-1,1)=0.
      W(I-1,1)=0.
    9 CONTINUE
      RETURN
      END
```

Calculation of the Pressure Gradient

Calculation of the pressure gradient was accomplihed by first solving the potential-flow problem as outlined in the text, and then using Eq. 80 to determine the necessary pressure term. The potential, or inviscid-,

assumption asserts that the velocities are derived from a potential; that is:

$$U_p = \frac{\partial \phi}{\partial x}$$

$$W_p = \frac{\partial \phi}{\partial z}$$

Using continuity, we establish that:

$$\frac{\partial^2 \phi}{\partial x^2} + \frac{\partial^2 \phi}{\partial z^2} = 0$$

This equation is solved numerically, assuming that U_p is constant at the side boundaries of the flow field, and at the top of the flow field, and that the vector velocity, $U_p \hat{i} + W_p \hat{j}$, is parallel to the assumed surface (see text). A computer program has been developed to accomplish this solution. As this is an elliptic partial-differential equation, the solution technique is iterative. We have assumed finite difference approximations to the derivatives involved, and proceeded through the flow field calculating the potential, ϕ, point by point much as was done in the concentration cases of the previous appendicies. When a stable value for ϕ was obtained, pressure gradients were calculated from the above equations, and Eq. 80. These were punched on cards and read into the program solving the conservation of momentum equation, to be discussed later.

```
      PROGRAM PRESS (INPUT,OUTPUT)
      DIMENSION P(50,50),ZE(50),DZ(50),PRES(50,20),JS(50)
      READ 1,N,M,IF,ITR,H,HK,W,UD
    1 FORMAT (4I4,4F10.4)
C HERE P IS THE MATRIX USED FOR PHI, ZE IS THE SURFACE
C THAT THE FLOW IS ASSUMED TO BE OVER, DZ IS ITS
C DERIVATIVE, PRES IS THE FINAL MATRIX IN WHICH THE
C PRESSURE GRADIENT WILL BE STORED, JS IS A LINEAR
C ARRAY IN WHICH INTGER VALUES OF ZE WILL BE STORED,
C N AND M ARE THE HORIZONTAL AND VERTICAL DIMENSIONS
```

```
C OF THE FLOW FIELD, IF IS THE X STEP AT WHICH THE
C BARRIER IS PLACED, ITR IS THE NUMBER OF ITERATIONS
C WHICH THE PROGRAM WILL CALCULATE, H AND HK ARE THE
C HORIZONTAL AND VERTICAL STEP LENGTHS, W IS THE
C SUCESSIVE OVER-RELAXATION FACTOR, AND UD IS THE
C VALUE OF THE VELOCITY AT THE BOUNDARIES OTHER THAN
C THE SURFACE.
      DO 42 I=1,N
      DO 42 J=1,M
      PRES(I,J)=0.
   42 CONTINUE
      NM=N-1
      MM=M-1
      DO 3 I=1,N
      X=(I-IF)*H
      IF (X) 4,4,5
    4 ZE(I)=.65*(1.03516/EXP(.4194*(X-.3261)**2))+.01
      DZ(I)=.65*1.03516*.4194*2*(.3261-X)/EXP(.4194*(X
     1 -.3261)**2)
      JJ=ZE(I)+1.
      JS(I)=JJ
      DO 6 J=JJ,M
      P(I,J)=I*UD*H
    6 CONTINUE
C THIS IS AN INITIAL GUESS AT THE VALUES OF P.
      GO TO 3
    5 ZE(I)=1.59*.65/EXP(.0071*(ABS(X-4.7))**2.7136)+.
     1 01
      JJ=ZE(I)+1.
      JS(I)=JJ
      DO 8 J=JJ,M
      P(I,J)=I*UD*H
    8 CONTINUE
      IF (X-4.7) 10,10,9
   10 DZ(I)=1.59*.65*.0071*2.7136*(ABS(X-4.7))**1.7136
     1 /EXP(.0071*(ABS(X-4.7))**2.7136)
      GO TO 3
    9 DZ(I)=1.59*.65*.0071*2.7136*(ABS(X-4.7))**1.7136
     1 /EXP(.0071*(ABS(X-4.7))**2.7136)*(0-1)
    3 CONTINUE
C THIS COMPLETES THE SET UP OF THE SURFACE BOUNDARY
C CONDITION.
      HOLD=0.
   22 DO 11 II=1,ITR
      C=-2*UD*H
      CALL PHI (W,H,HK,P(2,1),P(1,2),P(1,1),P(1,2),P(2
     1 ,1),C)
      DO 12 J=2,MM
      CALL PHI (W,H,HK,P(2,J),P(1,J-1),P(1,J),P(1,J+1)
     1 ,P(2,J),C)
   12 CONTINUE
      CALL PHI (W,H,HK,P(2,M),P(1,M-1),P(1,M),P(1,M-1)
```

```
     1 ,P(2,M),C)
C THIS CALCULATES THE LEFT BOUNDARY.
      DO 13 I=2,NM
      JJ=ZE(I)+1.
      Z=ZE(I)-HK*JJ
      P(I,JJ)=P(I,JJ)-W/(Z/HK**2-1./(2.*HK))*(DZ(I)/(2
     1 *H)*P(I-1,JJ+1)+(Z/HK**2-1./(2*HK))*P(I,JJ)-2*Z
     2 /HK**2*P(I,JJ+1)+(1./(2*HK)+Z/HK**2)*P(I,JJ+2)-
     3 DZ(I)/(2*H)*P(I+1,JJ+1))
      JJ=JJ+1
      C=0.
      DO 16 J=JJ,MM
      CALL PHI (W,H,HK,P(I-1,J),P(I,J-1),P(I,J),P(I,J+
     1 1),P(I+1,J),C)
   16 CONTINUE
      CALL PHI (W,H,HK,P(I-1,M),P(I,M-1),P(I,M),P(I,M-
     1 1),P(I+1,M),C)
   13 CONTINUE
C THIS CALCULATES THE MAIN BODY OF THE FLOW FIELD.
      C=2*H*UD
      CALL PHI (W,H,HK,P(N-1,1),P(N,2),P(N,1),P(N,2),P
     1 (N-1,1),C)
      DO 19 J=2,MM
      CALL PHI (W,H,HK,P(N-1,J),P(N,J-1),P(N,J),P(N,J+
     1 1),P(N-1,J),C)
   19 CONTINUE
      CALL PHI (W,H,HK,P(N-1,M),P(N,M-1),P(N,M),P(N,M-
     1 1),P(N-1,M),C)
C THIS CALCULATES THE RIGHT BOUNDARY.
   11 CONTINUE
```

At this point in the program the values of Φ have been calculated. The remainder of the program simply calculates first the values of U_p and W_p using finite difference approximations to the derivatives given before, and then the values of the pressure gradient using Eq. 80, and again, finite difference approximations to the derivatives involved.

Calculation of Eddy Diffusivities

Having the velocities and pressure gradients, we are now able to solve the conservation of momtumequation to arrive at a characterization of the turbulent transfer terms. This allowed us to arrive

at approximations to the eddy diffusivities. Using the finite difference values of the velocity and pressure gradient, we were able to simply plot a grid of values of T from Eq. 86. As outlined in the text we then used the method of characteristics to achieve a solution. This was done by a simple numerical intergration along characteristic lines. Although the actual boundary condition used was specifying that τ drop to background levels at sufficiently large heights, this was implemeted by inputting a value of τ at the surface, such that a sufficiently small value would be attained far away from the surface. This was found necessary to keep from making the flow field so large that calculation would become overly cumbersome. The numerical integration was accomplished by a computer program in which the values of T were read in on cards. The program then started with ground-level boundary values of τ and integrated point by point along the characteristic lines to calculate τ at all points in the flow field.

```
      PROGRAM DIFF (INPUT,OUTPUT)
      DIMENSION T(80,80),BC(200)
      READ 11,N,M,NBC,H,HK
   11 FORMAT (3I4,2F10.4)
C HERE T IS THE T OF EQ. 80, BC IS AN ARRAY HOLDING
C THE BOUNDARY VALUES OF TAU, N AND M ARE THE DIMENSIONS
C OF THE FLOW FIELD, NBC IS THE NUMBER OF BOUNDARY
C VALUES READ IN, AND H AND HK ARE THE STEP LENGTHS
C IN THE HORIZONTAL AND VERTICAL DIRECTIONS.
      KF=H/HK
      NM=N-1
      MM=M-1
      DO 54 I=1,N
      READ 55 (T(I,J),J=1,M)
   55 FORMAT (1X,8F10.4)
   54 CONTINUE
C THE VALUES OF T ARE READ IN.
      DO 40 I=1,NBC
      READ 41, BC(I)
   41 FORMAT (1X,1F10.4)
```

```
   40 CONTINUE
C THE BOUNDARY VALUES OF TAU ARE READ IN.
      DO 62 I=2,NM
      J=1
      L=I
      T(I,J)=-T(I,J)*H+BC
   65 IF (L-2) 62,62,63
   63 IF (J-MM) 64,62,62
   64 L=L-1
      J=J+1
      T(L,J)=T(L+1,J-1)-T(L,J)*H
      GO TO 65
   62 CONTINUE
C THIS IS THE BASIC INTEGRATION. SINCE THE CHARACTER-
C ISTIC LINES SLOPE TO THE LEFT , PARTS OF THE FLOW
C FIELD MUST STILL BE CALCULATED. THIS IS DONE BY
C ESTABLISHING BOUNDARY VALUES ON THE RIGHT VERTICAL
C BOUNDARY.
      DO 68 J=2,M
      L=NM
      K=J
      T(L,K)=-T(L,K)*H+BC(NM+J-1)
   69 IF (K-MM) 70,68,68
   70 L=L-1
      K=K+1
      T(L,K)=T(L+1,K-1)-T(L,K)*H
      GO TO 69
   68 CONTINUE
      DO 28 I=1,N
      PRINT 26,(T(I,J),J=1,M,KF)
   26 FORMAT (1X,20F6.2)
   28 CONTINUE
      STOP
      END
```

Now that the turbulent terms are calculated, we may establish the eddy diffusivities from Eq. 95.

Calculation of Concentration Profiles

The calculation of concentrations differs very little from the previous cases. The primary differences are that here the surface is considered to be the top of the cavity instead of the ground, and the vertical velocity is now calculated by the previously presented subroutine, not by the concentra-

tion program itself. As it differs so little from the discontinuity case, the concentration program is not presented here. The iteration scheme is exactly the same as the discontinuity case, the only difference being the boundaries inside which it applies.

TECHNICAL INFORMATION DIVISION
LAWRENCE BERKELEY LABORATORY
UNIVERSITY OF CALIFORNIA
BERKELEY, CALIFORNIA 94720